THE JOURNAL OF BIOLOGICAL CHEMISTRY
Vol. 278, No. 4, Issue of January 24, pp. 2604–2613, 2003

*Printed in U.S.A.*

# Functional Analysis of a Divergent System II Protein, Ccs1, Involved in *c*-Type Cytochrome Biogenesis*[S]

Received for publication, August 23, 2002, and in revised form, October 16, 2002
Published, JBC Papers in Press, November 9, 2002, DOI 10.1074/jbc.M208652200

**Beth Welty Dreyfuss, Patrice P. Hamel, Stacie S. Nakamoto, and Sabeeha Merchant‡**

*From the Department of Chemistry and Biochemistry, UCLA, Los Angeles, California 90095-1569*

**The *Ccs1* gene, encoding a highly divergent novel component of a system II type *c*-type cytochrome biogenesis pathway, is encoded by the previously defined *CCS1* locus in *Chlamydomonas reinhardtii*. *phoA* and *lacZα* bacterial topological reporters were used to deduce a topological model of the *Synechocystis* sp. 6803 Ccs1 homologue, CcsB. CcsB, and therefore by analogy Ccs1, possesses a large soluble lumenal domain at its C terminus that is tethered in the thylakoid membrane by three closely spaced transmembrane domains in the N-terminal portion of the protein. Molecular analysis of *ccs1* alleles reveals that the entire C-terminal soluble domain is essential for Ccs1 function and that a stromal loop appears to be important *in vivo*, at least for maintenance of Ccs1. Site-directed mutational analysis reveals that a single histidine ($His^{274}$) within the last transmembrane domain, preceding the large lumenal domain, is required for *c*-type cytochrome assembly, whereas an invariant cysteine residue ($Cys^{199}$) is shown to be nonessential. Ccs1 is proposed to interact with other Ccs components based on its reduced accumulation in *ccs2*, *ccs3*, *ccs4*, and *ccsA* strains.**

Universal to all energy-transducing membrane systems is the presence of *c*-type cytochromes on the *p*-side of the membrane, which corresponds to the plastid lumen, the mitochondrial intermembrane space, and the bacterial periplasm. Their distinguishing feature is the covalent attachment of the heme prosthetic group through thioether linkage(s) between one or, in most cases, both of the cysteine residues lying in the C*XX*C(H/K) motif of the apocytochrome and the vinyl groups of heme. Genetic approaches to identify *c*-type cytochrome-specific assembly factors led to the conclusion that at least three distinct systems (I, II, and III) evolved for the conversion of these molecules to their holoforms (for review see Refs. 1–5). System I, also referred to as the Ccm[1] pathway, is known from extensive studies in α- and γ-proteobacterial models such as *Rhodobacter capsulatus* (6–9), *Bradyrhizobium japonicum* (10–12), *Paracoccus denitrificans* (13–16), and *Escherichia coli* (17, 18). 9 to 12 genes, whose products are dedicated to the assembly of all *c*-type cytochromes, define the Ccm pathway (for review see Refs. 1, 19, and 20). The Ccm[2] proteins include subunits for a putative ABC-type transporter (6, 7, 10, 14, 21–23), components of a cytochrome biogenesis-specific thiol metabolism sub-pathway (8, 19, 24–29), a putative cyt *c*/heme lyase (30), a unique periplasmic heme chaperone (18, 31) and its accompanying heme delivery component (32–35). In contrast, system III, which was discovered through extensive genetic analysis in fungi and seems to be restricted to the mitochondria of vertebrates and invertebrates, is a minimal system with a single component, the so-called cytochrome *c* and $c_1$ heme lyases (CCHL and $CC_1HL$) (36–39). The system III CCHLs display no sequence similarity to system I and system II components; the similarity between individual CCHLs is itself limited to the occurrence in their N-terminal domains of between one to three CPV motifs that are believed to be involved in an interaction with heme (40, 41).

System II, the subject of this paper, operates in plastids, cyanobacteria, and some bacteria (42). Genetic studies in the green alga *Chlamydomonas reinhardtii* have assigned up to six loci, plastid *ccsA* and nuclear *CCS1* to *CCS5* (43–45), to the maturation of chloroplast *c*-type cytochromes, membrane-bound cyt *f* and soluble cyt $c_6$. Two of these have been identified molecularly. CcsA, encoded by the *ccsA* locus (46), is a multiple membrane-spanning protein and contains the tryptophan-rich motif with the "WWD" signature first noted in CcmC and CcmF of system I (4, 21, 46), and Ccs1, which also displays characteristic features of a membrane protein (47). Ccs1 lacks any domains or structural features that might speak to a specific chemical function, and it appears to be unique to system II (20, 47).

Genetic studies in *Bacillus subtilis* and *Arabidopsis thaliana*, and functional genomics in *Bordetella pertussis*, revealed two additional components required for *c*-type cytochrome biogenesis in system II (48–50). One is a membrane-anchored thioredoxin-like protein with its thiol-reducing active site on the *p*-side of the membrane, called ResA/HCF164/CcsX, respectively (49–51), and the other is CcdA, discovered originally in *B. subtilis* (48, 52). CcdA corresponds to the central portion of DipZ/DsbD, which functions in transmembrane thiol redox metabolism in *E. coli* and other bacteria (53). In *B. pertussis*, DipZ/DsbD is believed to function together with CcsX to provide the reductant to reduce apocytochromes, either directly or indirectly, on the *p*-side of the membrane before attachment of heme to the cysteinyl thiols (49).

* This work was supported by National Institutes of Health Grant GM48350, NRSA Grant GM17483 from the National Institutes of Health (to B. W. D.), American Heart Association Post-doctoral Fellowship 0120100Y (to P. H.), and a United States Public Health Service NRSA Award GM07185 from the National Institutes of Health (to S. S. N.). The costs of publication of this article were defrayed in part by the payment of page charges. This article must therefore be hereby marked "*advertisement*" in accordance with 18 U.S.C. Section 1734 solely to indicate this fact.

[S] The on-line version of this article (available at *http://www.jbc.org*) contains Experimental Procedures, Figs. 1 and 2, and Table I.

‡ To whom correspondence should be addressed: Dept. of Chemistry and Biochemistry, UCLA, Box 951569, Los Angeles, CA 90095-1569. Tel.: 310-825-8300; Fax: 310-206-1035; E-mail: merchant@chem.ucla.edu.

[1] The abbreviations used are: Ccm, cytochrome *c* maturation; ccs, cytochrome *c* synthesis; Chl, chlorophyll; cyt, cytochrome; $Me_2SO$, dimethyl sulfoxide; RT, reverse transcription.

[2] For consistency, the *ccm* nomenclature for the system I genes will be employed throughout.

For CcsA, CcdA, or CcsX, conserved sequence motifs suggest functional domains, but this has not been the case for Ccs1, which is a highly divergent protein. Its apparently essential function in popular bacterial model systems has hindered mutational analysis (54). Nevertheless, the fact that the cytochrome assembly pathways operate on multiple, divergent apoprotein substrates (two in *C. reinhardtii* and up to seven in *B. pertussis* (42)) may be suggestive of a direct interaction between Ccs1 and the apocytochrome. The limited sequence relationship among Ccs1 proteins would therefore be a consequence of co-evolution with the highly divergent apocytochromes. In this work, we undertake molecular and functional analyses of Ccs1. First, we confirm through molecular complementation that mutants previously assigned to the *CCS1* locus are the result of lesions in the *Ccs1* gene. Molecular characterization of each *ccs1* allele reveals that a stromal loop appears to be functionally important, at least for the stability of Ccs1 *in vivo*. Second, we suggest that Ccs1 functions together not only with CcsA, as has been shown in an accompanying paper (55), but also with multiple other Ccs components to form a "CCS complex." Third, we undertake membrane topological analysis and site-directed mutagenesis to generate a functional model for Ccs1. We find that a single histidine residue, located within the final transmembrane domain, preceding the large soluble domain is necessary for *c*-type cytochrome assembly in chloroplasts.

## EXPERIMENTAL PROCEDURES

*Strains and Culture Conditions*—*C. reinhardtii* wild-type strain CC-125 (MT+) and mutant strains *ccsA-B6* (CC-2695/CC-2934), *ccs1-ac206* (CC-939/CC-1112), *ccs1-2* (CC-3422/3423), *ccs1-3* (CC-3424/CC-3425), *ccs1-4* (CC-3426), abf3 (now *ccs1-5*::*NIT1*), *ccs2-1* to *ccs2-5* (CC-3428 to CC-3437), *ccs3-F18* (CC-3092/CC-3093), *ccs4-F2D8* (CC-3910/CC-3720), and *ccs5-1*::*ARG7* (CC-3717/CC-3718), described previously (4, 43, 45, 47, 56, 57), can be obtained from the Chlamydomonas Genetics Center (Duke University, Durham, NC). Arginine-auxotrophic strain *arg7cw15A* used for insertional mutagenesis was obtained from Prof. J.-D. Rochaix, University of Geneva, Switzerland. Wild-type strains were grown at 22–25 °C in TAP medium (58) under cool fluorescent lights (15–125 $\mu$mol $m^{-2}$ $s^{-1}$) with agitation (225 rpm). Mutant strains were grown under the same conditions, except that the illumination was always reduced (15–25 $\mu$mol $m^{-2}$ $s^{-1}$). The C. *reinhardtii* mutant *y-1* (yellow-in-the-dark; CC-735) strain was grown in TAP medium at 22 °C, wrapped in aluminum foil when necessary to prevent exposure to light. To de-green light-exposed green cells, one-half of the culture was diluted every day into fresh TAP medium. In 10 days green cells were de-greened to a Chl concentration of 0.029 $\mu$g/ml. To re-green the cells (to a Chl concentration of 3.6 $\mu$g/ml), the flasks were unwrapped and exposed to light (100–125 $\mu$mol $m^{-2}$ $s^{-1}$) at 22 °C.

*Insertional Mutagenesis and Identification of ccs Mutants*—*ccs1-6*::*ARG7* strain was generated by insertional mutagenesis as described previously (45). Briefly, *arg7cw15A*-recipient cells were transformed with *Eco*RI-linearized pARG7.8$\phi$3 by the glass bead transformation method (59, 60). Arginine prototrophic colonies were screened based on their variable fluorescence to identify candidate mutants blocked on the reducing side of Photosystem II (61). Candidate *ccs* mutants were screened for accumulation of holocyt *f* and holocyt $c_6$ by heme staining and immunoblot analysis as described below. The *ccs1-6*::*ARG7* strain was deposited into the Chlamydomonas Genetics Center (CC-3715/CC-3716).

*Complementation of ccs1 Strains*—*ccs1* strains grown in TAP medium (3–7 $\times$ $10^6$ cells/ml) were collected by centrifugation, 1,500 $\times$ *g* for 5 min, and used directly for transformation (*ccs1-6*::*ARG7*) after resuspension in TAP medium (2 $\times$ $10^8$ cells/ml) or (for strains *ccs1-ac206* and *ccs1-2* through *4*) were resuspended in autolysin (prepared according to Ref. 62) at 2 $\times$ $10^8$ cells/ml and incubated for 30–45 min to digest away the cell wall, after which autolysin was diluted by addition of 40 ml of TAP medium. The cells were recovered by centrifugation at 1,500 $\times$ *g* for 5 min. For glass bead transformation (60), 0.3 ml of cells were vortexed for 15 s in the presence of 0.3 mg of acid-washed glass bead and DNA. 1 $\mu$g of *Sal*I-linearized wild-type p*Ccs1*-2 DNA (simply referred to as p*Ccs1* for remainder of paper (47)) was used for complementation transformations. Co-transformation experiments included the addition of 1 $\mu$g of *Eco*RI-linearized pSP109 encoding the *ble* marker (63). 1 $\mu$g of *Eco*RI-linearized pTZ18U was used in control transformation reactions to assess the frequency of reversion. Vortexed cells were diluted in 10 ml of TAP and transferred to 50-ml flasks for recovery overnight in a shaking incubator. Cells were harvested by centrifugation and resuspended in 1 ml of minimal medium without acetate (58). 0.5 ml of cells were plated on minimal agar plates and incubated at 50–125 $\mu$mol $m^{-2}$ $s^{-1}$ until photosynthetic colonies appeared (about 1–2 weeks). The remaining 0.5 ml of cells were plated onto TAP + zeomycin (Zeocin™, Invitrogen) (10 $\mu$g/ml) agar plates and incubated at 50–125 $\mu$mol $m^{-2}$ $s^{-1}$ until zeomycin-resistant transformants appeared (about 2–3 weeks). For the "empty vector" control transformations, the entire mix was plated onto minimal agar plates for selection for phototrophic growth.

The presence of introduced *Ccs1* sequences was confirmed by amplification of the integrated p*Ccs1* DNA using a gene-specific primer (CCS1–7; see Table I of the Supplemental Material for all primers) and the Universal M13 −20 primer specific for the vector. 7 $\mu$l of genomic DNA, prepared as described previously (64), was amplified using *Taq* DNA polymerase in the presence of 5% $Me_2SO$. Amplification conditions were 94 °C for 5 min prior to addition of polymerase, 25 cycles of 94 °C for 1 min, 52 °C for 45 s, 72 °C for 1 min, with a final 5-min extension at 72 °C.

*Protein Preparation and Analysis*—Cytochromes were detected after freeze-thaw fractionation and analysis of electrophoretically separated supernatant and pellet fractions by immunodecoration or by heme staining as described previously (43, 47, 65). Enriched thylakoid membrane fractions were prepared from sonicated cell lysates and analyzed immediately by denaturing PAGE according to Ref. 43. To increase efficiency of transfer of electrophoretically separated enriched thylakoid membrane proteins, 0.01% SDS was added to the transfer buffer (25 mM Tris, 192 mM glycine, 20% methanol). Enriched thylakoid membrane proteins were transferred at 50 V, 4 °C for ~2 h to 0.2-$\mu$m polyvinylidene difluoride membranes (Immobilon $P^{SQ}$, Millipore Corp., Bedford, MA). Polyclonal antisera raised against *C. reinhardtii* cytochrome $c_6$ (1:1000), cytochrome *f* fusion protein (1:1000) (66), and Trx-Ccs1 fusion protein (1:100) (see Experimental Procedures in the Supplemental Material) were used for detection of cyt $c_6$, cyt *f*, and Ccs1, respectively. Bound antibodies were detected chromagenically using alkaline phosphatase-conjugated secondary antibodies.

*Southern Blot Analysis*—3 $\mu$g of genomic DNA (see the Experimental Procedures for isolation in the Supplemental Material) was digested with restriction enzymes and analyzed by Southern blot hybridization. For strains *ccs1-ac206* and *ccs1-1*, the probe was prepared using Genesis non-radioactive nucleic acid labeling kit (Roche Molecular Biochemicals), hybridized, and detected chromogenically following the manufacturer's procedure. For strains *ccs1-3*, *ccs1-4*, and the insertional mutant, *ccs1-6*::*ARG7*, the probe was prepared and detected as described previously (67, 68).

*Sequencing of ccs1 Alleles and CC125*—Genomic DNA from *ccs1-ac206*, *ccs1-2*, *ccs1-3*, *ccs1-4,* and CC125 strains representing ~4 kb containing Ccs1 encoding DNA was sequenced. Sequences representing both DNA strands were obtained for the entire region from CC125. For the mutant alleles, the entire gene except intron 7 was sequenced. *CCS1* was amplified from genomic DNA in five fragments (Fig. 1*B*) by using primers sets A = CCS1–1 + CCS1–10, B = CCS1–2 + CCS1–9, C = CCS1–3 + CCS1–12, D = CCS1–4 + CCS1–11, and *intron 7* = CCS1–17 + CCS1–20 using either *Taq* DNA polymerase or Expand™ DNA polymerase (Roche Molecular Biochemicals). Amplification reactions (25 $\mu$l) contained 0.2 mM dNTPs, 0.64 pmol of each primer, 1.5 mM $MgCl_2$, 5% $Me_2SO$ in addition to the manufacturer's recommended components. Reactions were preheated at 94 °C for 2 min, prior to the addition of the polymerase, followed by 30 cycles as follows: 94 °C for 30 s; 56 °C for 45 s; 72 °C for 1 min; with a final 7-min extension at 72 °C. Amplification products were gel-purified by the freeze-squeeze method (69), sequenced directly by dye termination cycle sequencing using 3′ dye-labeled dideoxynucleotide triphosphates according to the manufacturer's instruction, and run on an ABI PRISM™ DNA Sequencer (PerkinElmer Life Sciences). Sequences were compiled and compared using ABI PRISM™ AutoAssembler program (PerkinElmer Life Sciences). Mutations were confirmed by sequencing multiple independent amplification products.

*RNA Preparation and Analysis*—The procedure for RNA isolation has been described previously (70). The abundance of *Ccs1* mRNA was estimated by amplification of cDNA under conditions that were suitable for quantitative estimation of transcript abundance relative to *Cpx1* transcript abundance. Total RNA was treated with RQ1-DNase (Promega, Madison, WI), phenol/chloroform-extracted, and ethanol-precip-

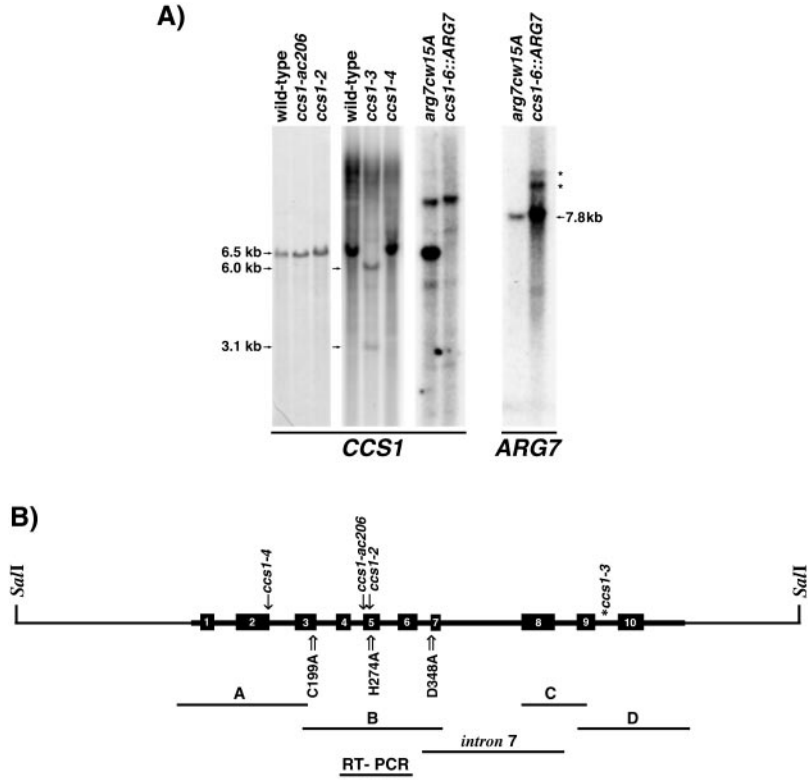


FIG. 1. **Southern analysis of DNA from *ccs1* strains and schematic map of *CCS1* loci.** *A*, approximately 3 $\mu$g of nucleic acids from wild-type, *arg7cw15A,* and *ccs1* strains was subjected to *Sal*I restriction enzyme digestion and analyzed for the presence of *Ccs1* or *Arg7* by Southern hybridization. For *Ccs1*, an ~2.3-kb *Xho*I fragment containing the entire *Ccs1* cDNA was labeled with digoxigenin-11-UTP (Roche Molecular Biochemicals) (for the blots shown for strains *ccs1-ac206* and *ccs1-2*) or with $^{32}$P-nucleotides by random priming. For strain *ccs1-6*::*ARG7*, a radiolabeled 6.5-kb *Eco*RI/*Sal*I fragment containing the *Ccs1* genomic DNA from p*Ccs1* or a 200-bp *Nco*I/*Sac*I exon 8 *Arg7*-specific probe from pKS-18 (86) was used. *B*, the *Ccs1* gene represented as a *thick line* on map of the 6.5-kb *Sal*I genomic fragment. Exons are represented as *numbered large black boxes.* The position of mutations in various *ccs1* alleles is indicated *above*, and the position of site-directed mutations is indicated *below* the gene structure schematic. *Lines below* the map represent genomic fragments that were amplified to determine the molecular lesions in various alleles. The fragment amplified for RT-PCR analysis is indicated.

itated as preparation for template for reverse transcription. Five $\mu$g of treated RNA was used as template for Moloney murine leukemia virus-reverse transcriptase according to the manufacturer's suggested procedure (Invitrogen) using pd$N_6$ random primers (Amersham Biosciences) (1.5 $\mu$l/20-$\mu$l reaction). Control reactions were set up with same input RNA but without the addition of reverse transcriptase (−RT). 1.5 $\mu$l of product was amplified directly in reactions (25 $\mu$l) containing 1.5 mM $MgCl_2$, 0.2 mM dNTPs, 0.64 pmol of each primer, 5% $Me_2SO$, and 1.25 units of *Taq* polymerase (Fisher) with other components as specified by the manufacturer of the enzyme. *Ccs1* transcripts or *Cpx1* transcripts were amplified with primer sets CCS1–5 and CCS1–6 (Fig. 1*B*) or CPX1–1 and CPX1–2, respectively (64). Amplifications conditions are as follows: 94 °C for 2 min; 30 cycles at 94 °C for 30 s, 50 °C for 30 s, 72 °C for 45 s and a final extension of 72 °C for 7 min (on a GeneAmp PCR system 2400; PerkinElmer Life Sciences). The yield of both products was dependent on the amount of input RNA (0.05–10 $\mu$g). The amount of pd$N_6$ primer was determined to be saturating for synthesis of the cDNA, and the subsequent amplification reaction was in the exponential stage up to 35 cycles. The presence of the H274A mutation was confirmed by *Sac*II digestion of the PCR product.

*Generation and Analysis of CcsB-phoA and CcsB-lacZ Topological Reporters*—Eight CcsB-PhoA translational fusions were generated by PCR amplification of various segments of the *Synechocystis ccsB* gene (slr2087) with *Pfu* polymerase. The p*ccsB*:*phoA* plasmids expressing translational fusions of CcsB to PhoA with fusions at positions 23, 67, 134, 225, 288, 349, 410, and 458 of the CcsB polypeptide were constructed as described in the Experimental Procedures of the Supplemental Material. CcsB-encoding PCR products were cloned into pRGK200 (8), in-frame with the downstream *phoA* gene encoding alkaline phosphatase to yield the series of *ccsB*:*phoA* fusion plasmids. The reciprocal *ccsB*:*lacZ*$\alpha$ fusions for all junctions were generated from the series of p*ccsB*:*phoA* plasmids by replacing a 2.6-kb *Sal*I-*Pst*I fragment including the entire *phoA* gene with a 0.7-kb PCR-amplified *lacZ* segment corresponding to the $\alpha$ fragment of $\beta$-galactosidase in-frame with the upstream CcsB moiety. Alkaline phosphatase and $\beta$-galactosidase activities of each CcsB-PhoA and CcsB-LacZ$\alpha$ fusion were measured for two different clones in three independent assays as described in the accompanying paper (55).

*Generation of Site-directed Mutant Strains*—$Cys^{199}$, $His^{274}$, and $Asp^{348}$ were each mutagenized to alanine by overlap extension PCR (71) using *Pfu* polymerase (Stratagene, La Jolla, CA) and complementary mutagenic primer C199A-1 and C199A-2, H274A-1 and H274A-2, and D348A-1 and D348A-2 (see details in Experimental Procedures of the Supplemental Material). All mutagenized fragments were subcloned into p*Ccs1* and sequenced to verify introduction of the desired mutation and absence of non-target mutations. In addition to the desired mutation, mutagenic primers also contained silent mutations, which were used to distinguish mutagenized DNA from wild-type DNA. For complementation experiments, 1 $\mu$g of *Sal*I-linearized mutant *Ccs1* plasmid DNA was transformed into *ccs1-6*::*ARG7* or *ccs1-4* as described above. Co-transformants of p*Ccs1*-H274A were generated by transformation of *ccs1-4arg7* strain after autolysin treatment with 1 $\mu$g of *Sal*I-linearized p*Ccs1*-H274A DNA and 1 $\mu$g of pARG7 as described above. Arginine prototrophs were selected by plating on TAP agar plates (−arginine). The presence of the mutated *Ccs1* gene was confirmed by amplification of the region containing the mutation followed by diagnostic restriction enzyme digestion of the amplification product.

## RESULTS

*The Ccs1 Gene Corresponds to the CCS1 Locus*—The *Ccs1* gene was cloned originally from strain abf3 (now renamed *ccs1-5*::*NIT1*). The strain was proposed to be defective in *c*-type cytochrome synthesis based on a hallmark pleiotropic deficiency in cyt *f* and cyt $c_6$ (47). Nevertheless, the relationship to previously characterized *CCS* loci (44) could not be ascertained by classical genetic methodologies because strain *ccs1-5*::*NIT1* could not mate. Therefore, we assigned the *Ccs1* gene to the *CCS1* locus. Southern analysis (Fig. 1*A*) showed the following: (i) the *ccs1-3* strain shows an RFLP relative to the wild-type (*i.e.* DNA from *ccs1-3* displays 6.0- and 3.1-kb *Ccs1* hybridizing bands instead of a single 6.5-kb hybridizing band in wild-type cells), and (ii) strain *ccs 1–6*::*ARG7* fails to show any hybridizable *Ccs1* sequences when probed with the entire 6.5-kb *Sal*I fragment containing the *Ccs1* gene (Fig. 1*A*) or even a larger 8-kb *Not*I fragment (data not shown). *ccs1-6*::*ARG7* appears to contain at least two copies of the integrated *Arg7* containing plasmid (Fig. 1*A,* marked with *asterisks*). The integrated *Arg7* copies behave as a single locus, because arginine prototrophy co-segregates with the mutant *ccs* phenotype (data not shown). We conclude that the phenotype of *ccs1-6*::*ARG7* results from the insertion of multiple *Arg7* sequences coupled with the deletion of the *Ccs1* gene.

To assign unequivocally the *Ccs1* gene to the *CCS1* locus, we tested all members of the *CCS1* complementation group, in-

TABLE I
*Complementation of ccs1 alleles by transformation with wild-type Ccs1 gene*

*ccs1* strains were transformed with either p*Ccs1* or vector DNA (pTZ18U) and selected for restoration of photosynthetic growth on minimal medium.

| Strain | p*Ccs1* | | pTZ18U | |
|---|---|---|---|---|
| | No. prototrophs[a,b] | No. transformations | No. prototrophs[a] | No. transformations |
| *ccs1-ac206* | 39[c] | 2 | 0[c] | 1 |
| *ccs1-3* | 112 | 5 | 0 | 4 |
| *ccs1-4* | ~300–600[b] | 4 | 0 | 4 |
| *ccs1-6*::*ARG7* | 99 | 3 | 0 | 2 |

[a] Average number of colonies. $6 \times 10^7$ cells were used per transformation experiment.
[b] The number of transformants varied depending on the batch of autolysin used to digest cell walls prior to glass bead transformation. For strain *ccs1-4*, the number of transformants obtained was very high, and the number of colonies was estimated.
[c] Prototrophs appeared as large well defined colonies rising up from lawn of very slowly growing cells. Lawn of slowing growing cells remained visible in plasmid control transformation experiment, but no prototrophic colonies were visible, even after 3 weeks of growth at 50–125 $\mu$mol $m^{-2}$ $s^{-1}$.

cluding four UV-generated mutants (*ccs1-ac206*, *ccs1-2* to *ccs1-4*) plus *ccs1-6*::*ARG7* by molecular complementation for restoration of phototrophic growth. For all alleles, transformation of the mutants with a plasmid containing 6.5 kb of genomic *Ccs1* DNA yielded phototrophic colonies on minimal medium (Table I). No phototrophic colonies were observed when the stains were transformed with empty vector DNA. When individual phototrophic colonies were tested for the presence of the integrated plasmid copy of *Ccs1*, all were found to be positive relative to the untransformed recipient (representative examples in Fig. 2*A*). Strain *ccs1-2* could not be tested directly for rescue with p*Ccs1* because it carries a leaky allele and displays appreciable growth on minimal medium. Therefore, we introduced p*Ccs1* by co-transformation with the dominant *ble* marker, conferring resistance to zeomycin. Co-transformants of interest were identified among the zeomycin-resistant colonies by specific amplification of the introduced copy of *Ccs1*. These co-transformants, *ccs1-2* (p*Ccs1*), displayed wild-type phototrophic growth and fluorescence rise and decay kinetics (not shown). Several rescued colonies from each transformation were tested by immunoblot and heme stain analysis and found consistently to accumulate wild-type (or near wild-type) levels of cyt *f* (representative transformant shown in Fig. 2*B*). Occasionally, slight variability in holocyt *f* abundance was noted in a particular strain, but this was attributed to positional effects resulting from unique integration of p*Ccs1* in individual transformants. Because selection for phototrophic growth relies only on restoration of cyt *f* function, complemented transformants were also tested for cyt $c_6$ accumulation. As expected, copper-deficient transformants accumulated holocyt $c_6$ to approximately wild-type levels, confirming that the transformants were rescued for Ccs function.

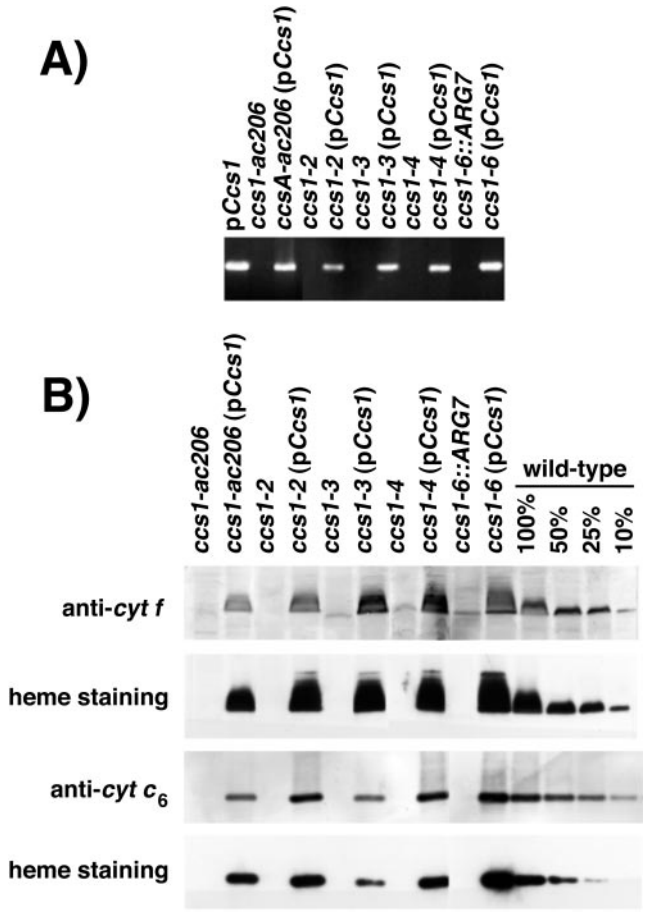


FIG. 2. **Complementation of *ccs1* strains by transformation with wild-type genomic *Ccs1* DNA.** *A*, genomic DNA from *ccs1* strains and representative complemented transformants was amplified. The introduced p*Ccs1* DNA was distinguished by using a *Ccs1*-specific primer (CCS1–7) and a plasmid specific primer (Universal). p*Ccs1* was amplified in parallel to generate a product standard. *B*, extracts were prepared from copper-deficient cultures of each strain. Proteins from the insoluble membrane fraction (equivalent to 5 $\mu$g of chlorophyll) were separated in a 12% polyacrylamide gel under denaturing conditions, and the immunoblots were probed with antiserum against *Chlamydomonas* cyt *f*. Total soluble proteins (equivalent to 5 $\mu$g of chlorophyll) were separated in 15% polyacrylamide gels under nondenaturing conditions, and immunoblots were probed with antisera against *Chlamydomonas* cyt $c_6$. Heme-containing proteins immobilized on the membranes were detected by chemiluminescence. Because cyt $c_6$ expression is strictly regulated by copper availability, the extent of holocytochrome $c_6$ accumulation reflects minor differences in cellular copper nutritional status (87).

*Ccs1 Accumulation during Cytochrome Biogenesis*—To monitor Ccs1 abundance, we raised antibodies against the putative C-terminal lumenal domain of Ccs1 (see below for topological model). The antiserum recognized a protein of ~60 kDa (Fig. 3). The signal is quite weak and is detected only when freshly prepared membranes were analyzed. When the membranes were purified on gradients or when they were stored (even frozen at −80 °C), the signal became weaker and was difficult to visualize over the noise. Therefore, for immunoblot analysis, we used a rapid method for preparing a thylakoid membrane-enriched fraction, which was solubilized directly and immediately used for electrophoretic separation.

Previously, we found that coprogen oxidase, a tetrapyrrole biosynthetic enzyme, was induced in copper deficiency, and we attributed this to an increased demand for heme synthesis when cyt $c_6$ was induced (72). Therefore, we wondered whether Ccs1 accumulation might similarly be affected by copper nutritional status. However, we noted that cells adapted to either copper-replete or copper-deficient conditions accumulate the same amount of Ccs1 (Fig. 3*A*). On the other hand, the abundance of Ccs1 did increase on a per cell basis as the culture grew from log phase to stationary phase (Fig. 3*B*). At low cell density, we also observed a faster migrating band (marked with

*faint arrow*) whose appearance correlated with cell density, *i.e.* more predominant in cultures in early exponential growth than stationary phase cultures (Fig. 3*B*). We know that the faster migrating band is Ccs1-specific because it is absent in immunoblots of *ccs1* null mutants (see Fig. 9). At present, it is unclear if the faster migrating molecule is a physiologically relevant species or simply represents a degradation product generated during sample preparation.

The *y-1* strain (deficient in the light-independent protochlorophyllide reductase, see Ref. 73) has been used as a model system to study thylakoid membrane biogenesis by light-initiated greening of de-greened cells (74–76). In contrast to chlorophyll proteins, cytochromes do accumulate in dark grown and non-green plastids (77), but their abundance increases along with other components of the thylakoid membrane as the de-greened cells re-assemble their photosynthetic apparatus (78, 79). We hypothesized that Ccs1 would be present in non-green plastids. As expected, both Ccs1 and cyt *f* are present in dark grown *y-1* cells. The abundance of both proteins increased in parallel to each other and with the synthesis of chlorophyll (Fig. 4). Nevertheless, although the accumulation of cyt *f* requires Ccs1 function, the accumulation of Ccs1 is independent of cyt *f*. For instance, a *petA* deletion mutant (FIEB1, 80) accumulates Ccs1 to wild-type levels (data not shown).

*Functional Analysis and Topology*—With the objective of

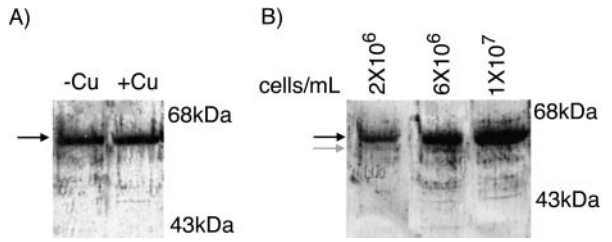


FIG. 3. **Abundance of Ccs1 under various growth conditions.** Enriched thylakoid membrane fractions (corresponding to 50 $\mu$g of Chl for each lane) from wild-type cultures were tested for the accumulation of Ccs1 by immunoblot analysis. Wild-type cells were grown in the presence or absence of copper (*A*) and to different cell densities (*B*). Solubilized proteins were separated by electrophoresis on SDS-containing polyacrylamide (10%) gels, transferred to polyvinylidene difluoride membranes, incubated overnight with anti-Ccs1 antisera, and detected chromogenically using an alkaline phosphatase-conjugated secondary antibody. *Arrows* indicate position of Ccs1-specific species. The anti-Ccs1 antiserum specifically recognizes a protein of ~60 kDa that is present in wild-type samples and absent in *ccs1* mutants (see Fig. 9).

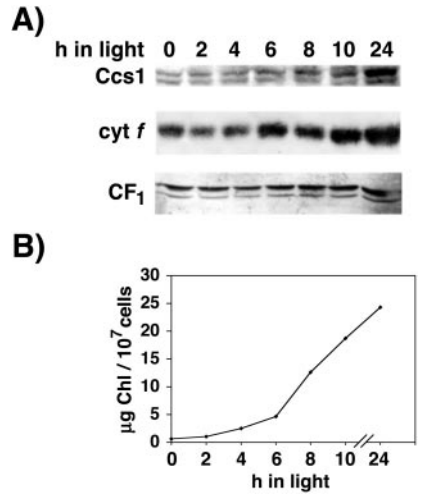


FIG. 4. **Ccs1 and cytochrome *f* accumulation during greening.** *A*, Ccs1, cyt *f,* and $CF_1$ (as loading control) were monitored during the greening of *y-1* (*yellow* in the *dark*) mutant cells. Enriched thylakoid membranes fractions were prepared after the indicated number of hours of light exposure. Protein samples corresponding to $5.25 \times 10^6$ cells per lane were separated electrophoretically on an 8.75% SDS-containing gel for immunoblot analysis. *B*, the parallel accumulation of Chl was determined by organic extraction of Chl and spectrophotometric quantitation.

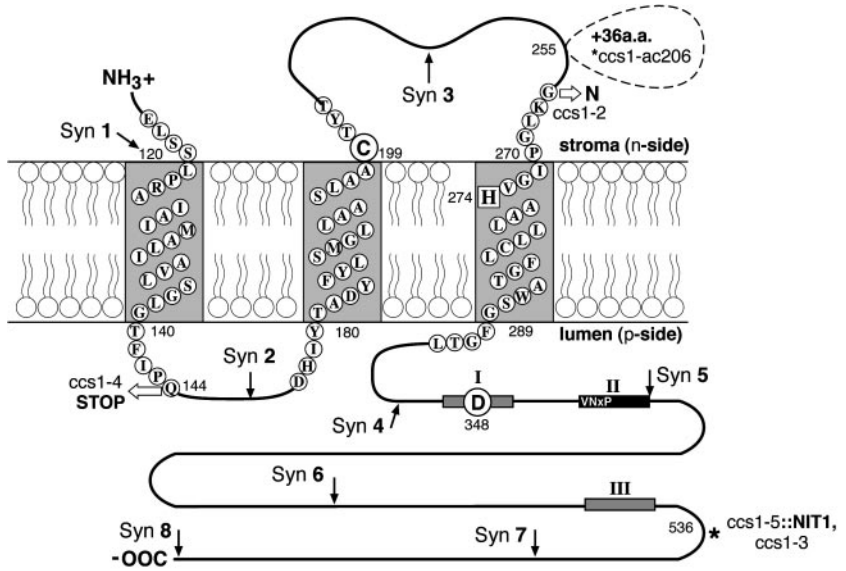


FIG. 5. **Topological arrangement of *Chlamydomonas* Ccs1 in the thylakoid membrane.** The predicted topology is based on *phoA* and *lacZ* fusion analysis of *Synechocystis* CcsB and the alignment of *C. reinhardtii* Ccs1 and *Synechocystis* CcsB sequences (see Supplemental Material Figs. 1 and 2). The equivalent positions of *Synechocystis* fusion constructs are indicated by *numbered arrows* (*Syn*1 through *Syn*8). This topology is consistent with the topological prediction based on the "positive-inside" rule (number of basic residues in loop 1: *C. reinhardtii* = +3, *Synechocystis* = +1. Number of basic residues in loop 2: *C. reinhardtii* = +12, *Synechocystis* = +14 (88)). The point mutations in *ccs1* alleles are indicated by *open arrows* at the position of the mutations. Residues altered by site-directed mutagenesis are shown as follows: C199A and D348A mutations, which did not result in a discernible phenotype are indicated by *circles.* The H274A mutation, which did result in a *ccs* phenotype, is indicated by a *square.* The relative position of the insertion of p*NIT1* in the insertional mutant *ccs1-5*::*NIT1* and the breakpoint in the *ccs1-3* allele is indicated by an * near the C terminus of protein. Regions within soluble lumenal domain displaying limited blocks of sequence conservation are indicated with *bold lines.* Region II containing an invariant signature motif VN*x*P, where *x* is a polar and generally positively charged residue (51 identifiable sequences, data base search May, 2002), is highlighted in *black*, whereas regions I and III showing less sequence conservation are highlighted in *gray* (see Supplemental Material Figs. 1 and 2 for alignment of Ccs1 sequences).

TABLE II
*Topology analysis of Synechocystis sp. PCC 6803 CcsB by phoA and lacZ fusion analysis*

Alkaline phosphatase and β-galactosidase activities of CcsB fusion proteins expressed in *E. coli* were measured as described under "Experimental Procedures." At least two representatives of each CcsB fusion were tested for activity. The value is indicated as the mean ± S.D. of three independent measurements for the two representatives. *n*-side and *p*-side correspond to the negative and positive side of the membrane, respectively.

| Fusion construct | Position in *CcsB*[a] | Position in *Ccs1*[b] | *phoA* activity | lacZ activity | Topology |
|---|---|---|---|---|---|
| | | | *Miller units* | *units* | |
| vector | | | 23 (±3) | 10 (±2) | |
| *Syn* 1 | 23 | 119 | 85 (±3) | 144 (±38) | *n*-Side |
| *Syn* 2 | 67 | 164 | 1368 (±124) | 10 (±3) | *p*-Side |
| *Syn* 3 | 134 | 231 | 65 (±7) | 58 (±7) | *n*-Side |
| *Syn* 4 | 225 | 323 | 1031 (±125) | 9 (±2) | *p*-Side |
| *Syn* 5 | 288 | 388 | 978 (±121) | 12 (±2) | *p*-Side |
| *Syn* 6 | 349 | 492 | 613 (±45) | 12 (±4) | *p*-Side |
| *Syn* 7 | 416 | 559 | 530 (±44) | 13 (±2) | *p*-Side |
| *Syn* 8 | 458 | 613 | 420 (±68) | 18 (±1.6) | *p*-Side |

[a] Position of actual fusion with CcsB from *Synechocystis* sp. PCC 6803.
[b] Equivalent position of CcsB fusion to Ccs1 from *C. reinhardtii* based on multiple alignment (See Supplemental Material Figs. 1 and 2).

TABLE III
*Complementation of ccs1 alleles by transformation with site-directed mutations in the Ccs1 gene*

Site-directed mutations in *Ccs1* were tested for their ability to complement *ccs1* strains and restore photosynthetic growth when selected on minimal medium.

| Mutation | Strain | No. prototrophs[a] | No. transformations |
|---|---|---|---|
| C199A | *ccs1-6*::*ARG7* | 150 | 5 |
| H274A | *ccs1-6*::*ARG7* | 0 | 3 |
| H274A | *ccs1-4* | 0 | 1 |
| D348A | *ccs1-6*::*ARG7* | 79 | 5 |

[a] Average number of colonies resulting from $6 \times 10^7$ cells per transformation experiment.

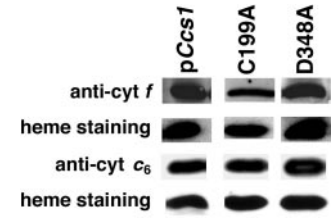


FIG. 6. **Accumulation of *c*-type cytochromes in C199A and D348A mutants.** Protein samples from cells transformed with plasmid carrying wild-type, C199A-encoding, or D348A-encoding copies of Ccs1 were prepared as described previously in Fig. 1 and analyzed by immunoblot or heme staining. For cyt *f*, membrane fractions were separated on a 10% SDS-containing polyacrylamide gel. An equivalent of 10 μg of Chl per sample was loaded. For cyt $c_6$, soluble protein samples were separated on a 15% native gel. An equivalent of 10 μg of Chl per sample was loaded.

deducing a functional model of Ccs1, we assembled a multiple alignment of all Ccs1-like sequences (see Supplemental Material Figs. 1 and 2). Based on these alignments, we predicted a topological arrangement of Ccs1 within the thylakoid membrane, and we also identified invariant residues (Fig. 5) (81). The topological predictions indicated that Ccs1 could contain three transmembrane segments in the N-terminal region of the protein followed by a large hydrophilic lumenal loop, followed by a fourth transmembrane span with a weak prediction rating at the C terminus (see hydropathy profiles in Ref. 47). To test the topology predictions, we used a cyanobacterial homologue of Ccs1, *Synechocystis* CcsB, in *phoA* and *lacZα* fusions. The relationship between *Synechocystis* CcsB and chloroplast Ccs1 is obvious, and the model of the cyanobacterial protein should be extendable to the chloroplast situation. Analysis of the fusion constructs confirmed three membrane spans domains clustered at the N terminus of the Ccs1 homologue (Table II). PhoA fusions on the *p*-side of the membrane, *Syn*2 and *Syn*4, show higher alkaline phosphatase activity compared with fusions *Syn*1 and *Syn*3 on the *n*-side. Conversely, *Syn*1 and *Syn*3 fusions are more active on the *n*-side as β-galactosidase fusions (Table II). Fusion constructs *Syn* 4-8 (where *Syn*8 is at the very C terminus of the protein) all show high alkaline phosphatase activity and conversely low β-galactosidase activity, which is consistent with the *p*-side location of the entire C-terminal domain. On this basis, we discount the weak prediction of a fourth transmembrane segment and favor the topology diagrammed in Fig. 5.

*An Essential Histidine*—Multiple alignment of Ccs1-like sequences at the outset of these experiments revealed very few residues in Ccs1 that are absolutely conserved (see Ref. 47) and hence might be catalytically significant. Because biochemical analysis of *ccs1* mutants suggested that Ccs1 participates in terminal steps of cytochrome synthesis involving attachment of heme to the apoprotein within the thylakoid lumen (43, 44), we considered that Ccs1 might be involved in substrate binding, either heme or apoprotein. Alignment of Ccs1 homologues highlighted three invariant residues, cysteine 199, histidine 274, and aspartic acid 348, with interesting functional groups and potential for interaction with heme. These three residues were chosen for site-directed mutagenesis and were changed to the neutral amino acid alanine. The corresponding alanine encoding mutated versions of *Ccs1* were then tested for their ability to rescue strain *ccs1-6*::*ARG7* for photosynthetic growth on minimal medium. Plasmids carrying the C199A and D348A mutations could complement *ccs1-6*::*ARG7*. Numerous photosynthetic colonies appeared after transformation (Table III) at frequencies comparable with wild-type (Table II). Representative C199A and D348A transformants were analyzed for the accumulation of holocyt *f* and holocyt $c_6$ (Fig. 6). As expected from their ability to grow on minimal medium, C199A and D348A transformants were fully capable of synthesizing holocyt *f*, and under copper-deficient growth conditions, both C199A and D348A transformants were able to synthesize holocyt $c_6$. Therefore, we conclude that cysteine 199 and aspartic acid 348 are not required for Ccs1 function under laboratory test conditions.

On the other hand, H274A failed to rescue either *ccs1-6*::*ARG7* or *ccs1-4* (which rescues at high frequency) (Table III), suggesting that histidine 274 is essential for Ccs1 function. To confirm the role of histidine 274, pH274A was introduced by co-transformation of *ccs1-4arg7* with p*Arg7*. Thirty-four H274A co-transformants were identified by specific amplification among 81 arginine prototrophs (two transformation experiments). Thirty of the 34 H274A co-transformants failed to show

photosynthetic growth on minimal medium and were unable to accumulate cyt *f* (see Fig. 7, *H274A lanes 1*, *2*, and *4* for representative examples). Four of the 34 H274A co-transformants displayed limited and spotty growth on minimal medium and accumulated ~5% of wild-type levels of cyt *f*, consistent with their limited photosynthetic capacity (see Fig. 7, *H274A lane 3* for a representative). Four of the H274A co-transformants were analyzed in more detail and confirmed by RT-PCR amplification followed by diagnostic restriction digestion of the product to express the H274A mutated version of the *Ccs1* mRNA (data not shown). All four confirmed H274A mutants accumulated very low levels of Ccs1 (~2–5% of wild type) (Fig. 7). Three of the four H274A mutants (1, 2, and 4) failed to accumulate either holocyt *f* or holocyt $c_6$, although very low levels of an anti-cyt *f* immunoreactive species still accumulated in these transformants. We concluded that the immunoreactive species is the apoprotein form because it is ~0.7 kDa smaller than native holocyt *f* (corresponding to loss of the heme group) and also the band does not stain for heme. The H274A transformant 3 that displays very limited growth on minimal medium appears to accumulate both the apoprotein and holoprotein forms of cyt *f* based on the observation of a doublet in Fig. 7. Only the upper band shows heme staining, confirming its identity as holocyt *f*. Interestingly, transformant 3 does not show any accumulation of either apo or holo form of cyt $c_6$. We conclude that the $His^{274}$ residue is important for Ccs1 function.

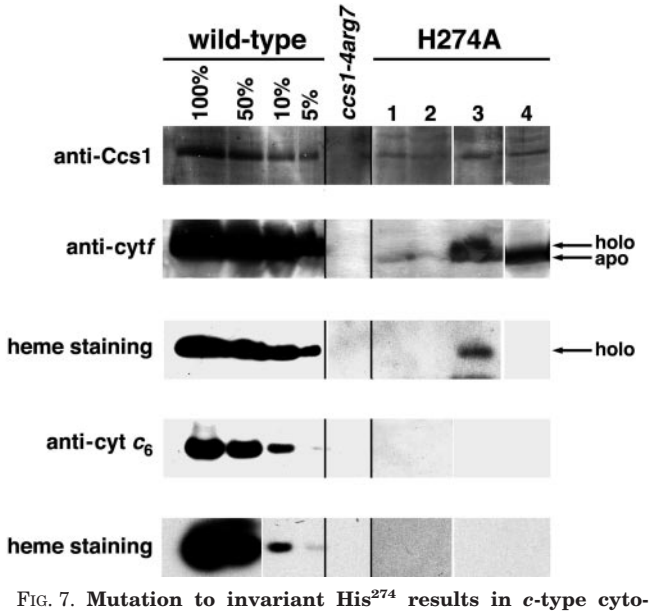


FIG. 7. **Mutation to invariant $His^{274}$ results in *c*-type cytochrome-deficient phenotype.** Enriched thylakoid membrane fractions were examined for the accumulation of Ccs1 and cyt *f* (as described previously). Soluble extracts from copper-deficient cultures were examined for the accumulation of cyt $c_6$. The presence holocytochromes in the samples was examined by heme staining (as described in Fig. 1). Exposures of heme staining representing equivalent intensities for wild-type samples are shown. Dilution series of wild-type, *ccs1-4arg7* (recipient strain for transformation), and four independent representative H274A site-directed mutant transformants are shown.

*Molecular Analysis of ccs1 Alleles*—The existing collection of *ccs1* alleles also provided an opportunity to distinguish functional domains in Ccs1. With this in mind, the mutations in each UV-generated *ccs1* allele were identified by sequencing the *Ccs1* genomic DNA from each strain (Fig. 1*B*) (GenBank™ accession numbers AY095299–AY095304). *Ccs1* was sequenced also from the corresponding wild-type strain, CC125 (GenBank™ accession number AY095298) (44). The mutations in the *ccs1* alleles are summarized in Table IV. In *ccs1-ac206*, the conserved guanine nucleotide at the 3′ splice site junction of intron 4 and exon 5 is mutated to A (Table IV). Because intron 4 is 108 nucleotides in length, failure to splice intron 4 from the *ccs1-ac206* mRNA would result in an mRNA encoding an additional 36 amino acids within the predicted stromal loop of Ccs1 (see Fig. 5). The longer species was not detected by RT-PCR; however, immunoblot analysis did reveal a slower migrating species, which could be a translation product from the unspliced longer transcript (discussed below). The *ccs1-2* phenotype results from a missense mutation wherein non-conserved glycine 260 is changed to asparagine, *ccs1-4* results from a nonsense mutation at codon 144, and the *ccs1-3* phenotype appears to be the result of a rearrangement within intron 9, which would be expected to destroy the very C-terminal 77

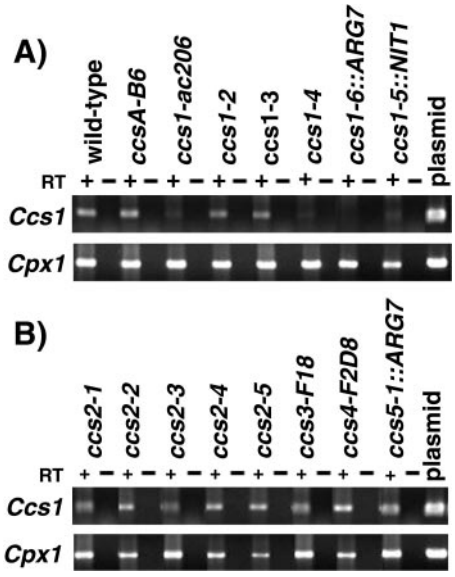


FIG. 8. **Expression of *Ccs1* in *ccs1* strains and other *ccs* mutants.** *C. reinhardtii* total RNA was isolated from wild-type or *ccs* mutants, digested with RQ1 DNase, and used as template for reversed transcription with random $pN_6$ primers. The cDNA corresponding to *Ccs1* transcripts were detected by amplification with CCS1–5 and CCS1–6 primers to yield a 345-bp product. A cDNA corresponding to *Cpx1* transcripts was amplified in parallel as an internal control using CPX1–1 and CPX1–2 primers resulting in a 634-bp product. Lanes marked *-RT* show the result of amplification reaction on the same RNA preparations but without reversed transcription. Plasmid DNA containing either *Ccs1* cDNA or *Cpx1* cDNA were used as templates for amplification with the same primers to generate a standard product (lane marked *plasmid*). *A*, *Ccs1* transcript abundance in various *ccs1* strains. *B*, *Ccs1* transcript abundance in other *ccs* mutants.

TABLE IV
*Summary of ccs1 mutations*

| Strain | Mutation | Predicted result on translation |
|---|---|---|
| *ccs1-ac206* | G1442/GTG → a1442/GTG | Failure to splice intron 4, potential read-through adding 36 amino acids between $Gln^{250}$ and $Val^{251}$ |
| *ccs1-2*[a] | G1470G1471 → AA | $Gly^{260}$ → N(AAC) |
| *ccs1-3* | Rearrangement within intron 9 | Truncation after 536 residues |
| *ccs1-4* | $Cys^{611}$ → Ala | $Gln^{144}$ → Stop (TAA) |

[a] Silent mutation at $Thr^{952}$ → Cys ($Y_{UAU}$ → $Y_{UAC}$) also observed in *ccs1-2* allele.

amino acids of the protein. The re-arrangement was verified by amplification (Fig. 1*B*) and was consistent with Southern analysis (Fig. 1*A*). Specifically, fragments A–C could be amplified from *ccs1-3* genomic DNA, and sequence analysis confirmed the wild-type sequence. Only the 5′ portion of fragment D could be amplified using a primer annealing within exon 9. Primers annealing downstream of exon 9 used in conjunction with the upstream CCS1–12 primer consistently failed to produce amplification products from *ccs1-3* DNA, whereas wild-type DNA yielded a product. On this basis, we placed the breakpoint for the genomic rearrangement in *ccs1-3* within intron 9 ~6.0 kb from the 5′ *Sal*I site. We noted that exon 10 could be amplified from *ccs1-3* to yield a product of the expected size, suggesting that the rearrangement event may be an inversion within the gene.

To assess the effect of each mutation on *Ccs1* expression, we assayed for the presence of *Ccs1* transcripts by a quantitative PCR-based method (Fig. 8). Reverse-transcribed cDNA was used as the template for amplification using primers that hybridized to exon 4 and exon 6. The amounts of *Ccs1* cDNAs were normalized against the amounts of *Cpx1* cDNAs, because *Cpx1* is expressed constitutively under these conditions, and the level of expression is unaffected in mutants. A product with the size expected for the mature *Ccs1* message was amplified from all strains (except *ccs1-6*::*ARG7* in which *Ccs1* has been completely deleted). Amplification products corresponding to templates derived from unspliced messages containing intron 4 and/or intron 5 were never observed from any RNA preparation. Strains *ccs1-2* and *ccs1-3* accumulate *Ccs1* transcripts to wild-type levels (Fig. 8*A*) as do *ccs2*, *ccs3*, *ccs4,* and *ccs5* alleles (Fig. 8*B*), but *ccs1-ac206* (mutation at conserved splice site G), *ccs1-4* (early nonsense), and *ccs1-5*::*NIT1* (insert in exon 10) accumulate only about 25% of wild-type levels of *Ccs1* transcripts. Surprisingly, the *ccs1-ac206* mRNA that accumulates seems to be spliced correctly, despite the mutation in intron 4. A product representing mRNA containing the unspliced intron 4 was never observed in the *ccs1-ac206* RNA population under the conditions used, even when intron 4-specific primers were used to target such a species (data not shown). The longer protein product (see below) implicates the existence of intron 4-containing mRNA in a translatable pool, but we conclude that the species must be short lived and hence not well represented in the mRNA pool. The decreased abundance of *ccs1-4* mRNA is not surprising because non-sense-mediated mRNA decay (82) has been observed previously in *Chlamydomonas* (65). Previously, we could not detect *Ccs1* mRNA in *ccs1-5*::*NIT1* by RNA blot analysis (47). In this work, a small steady state amount is implicated by the RT-PCR results, which indicates that *Ccs1* is still being transcribed in the insertional mutant.

The abundance of Ccs1 in the *ccs* mutants relative to wild-type cells was examined by immunoblot analysis of thylakoid membranes. The sensitivity was limited to detection of ~2–5% of wild-type levels of Ccs1 (Fig. 9*A*). Nevertheless, very low amounts of Ccs1 could clearly be seen in membranes from the missense *ccs1-2* strain. We suggest that the mutation must de-stabilize the protein, indicating the structural importance of the stromal loop. Membranes from *ccs1-ac206* contain a slower migrating form of Ccs1 in addition to very low levels of a wild-type sized Ccs1. The abundance of both forms is highly variable between sample preparations. The larger form is most likely the result of translational readthrough of the unspliced intron 4 in *ccs1-ac206*, which would add 36 amino acids to Ccs1, and the estimated size of the slower migrating form is consistent with a 4-kDa increase. Ccs1 was not detected in any other *ccs1* strain, which is expected from the nature of their molecular lesions. Interestingly, when we examined mutants at other *CCS* loci, we noted that strains *ccsA*, *ccs2*, *ccs3*, and *ccs4* each accumulated only 10–15% of wild-type levels of Ccs1 (Fig. 9*B*) even though Ccs1 mRNA accumulates to normal levels. The decreased accumulation of Ccs1 in these strains appears to be either translationally or post-translationally controlled (see "Discussion"). On the other hand, *ccs5–1*::*ARG7*, a leaky *ccs* strain that accumulates ~5–10% of wild-type levels of cyt *f* and cyt $c_6$ (45), accumulates wild-type amounts of Ccs1. Perhaps this suggests significant functional differences in the site of action of Ccs5 *versus* CcsA, Ccs1 through Ccs4.

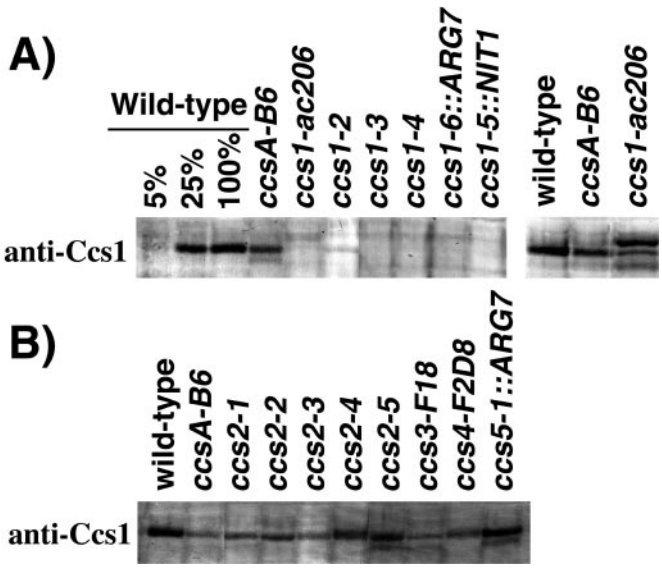


FIG. 9. **Abundance of *Ccs1* in various *ccs1* strains and other *ccs* mutants.** Enriched thylakoid membrane fractions (corresponding to 50 μg of chlorophyll) from wild-type or *ccs* strains were tested for the presence of Ccs1 by immunoblot analysis as described in Fig. 3. *A*, detection of Ccs1 in various *ccs1* strains. *B*, detection of Ccs1 in other *ccs* mutants.

## DISCUSSION

*Topology and Functional Importance of Domains within Ccs1*—Topology studies of *Synechocystis* sp. PCC 6803 CcsB (cyanobacterial homologue of plastid Ccs1) suggest that Ccs1/CcsB is anchored in the thylakoid membrane by three transmembrane domains within the N-terminal half of the protein, which places the C-terminal half as an extramembrane lumenal domain (Fig. 5). This topology differs slightly from the model for *B. pertussis,* CcsB (49), in which an additional transmembrane domain at the very C terminus of the protein was proposed, based on positive (albeit low) alkaline phosphatase activity for the full-length C-terminal *phoA* fusion. In our work, we have used both *phoA* and *lacZα* fusion analysis to strengthen the model that plastid/cyanobacterial type Ccs1/CcsB has only three transmembrane domains, and the entire C-terminal domain resides on the lumen side of the thylakoid membrane.

The topological model was a prerequisite for deriving insight from molecular analysis of the *ccs1* alleles and for building a functional model based on mutational analysis of conserved residues. Our first conclusion is that the stromal loop in Ccs1 is important (Fig. 5). The expected outcome of failure to splice intron 4 in strain *ccs1-ac206* is the insertion of 36 codons in the region of the mRNA corresponding to the stromal loop, and indeed, a protein of larger size was observed in *ccs1-ac206* (Fig. 9*A*). Strain *ccs1-ac206* also appears to produce normal sized Ccs1 at very low levels, probably from a pool of normally spliced intron 4 (see "Results"). However, holocytochromes do not accumulate (Fig. 2), which is consistent with previous studies

that showed by pulse-chase analysis that *ccs1-ac206* is completely incapable of holocytochrome formation (43). We conclude that the insertion of additional amino acids in the stromal loop renders the larger form non-functional and that this larger form must exert a dominant-negative effect on the lesser abundant normal Ccs1 population, suggesting Ccs1 associations with other Ccs components *in vivo*. Blue native-PAGE indicates that Ccs1 is found in an ~200-kDa CcsA-dependent Ccs complex in the thylakoid membrane (see accompanying paper (55)). This size is more than adequate to accommodate two subunits of Ccs1 and/or the products of other *CCS* loci. The decreased abundance of Ccs1 in *ccs2*, *ccs3,* and *ccs4* mutants (Fig. 9*B*) also argues in favor of Ccs1 interactions with additional Ccs components.

The importance of the stromal loop is underscored by molecular analysis of strain *ccs1-2* in which mutation of a single residue in the stromal loop, due to a conversion of a non-conserved glycine to an asparagine, results in dramatically reduced Ccs1 accumulation (~2% of wild-type levels). The altered residue lies a mere two amino acids away from a highly conserved pair of residues, $^{262}$KG$^{263}$ in the *Chlamydomonas* protein. The mutation must destabilize Ccs1 in the membrane, perhaps by affecting interactions with partner subunits. The G260N mutant form of Ccs1 is functional to the extent that it accumulates in the membrane (at least for assembly of holocyt *f*); between 1–5% of wild-type levels of holocyt *f* can be observed in thylakoid membranes from *ccs1-2* (44), and the strain grows to a limited extent on copper-replete minimal media. However, in copper-deficient medium, *ccs1-2* cannot synthesize holocyt $c_6$, and this is clearly evident in pulse-chase experiments (44). The separate effect of the *ccs1-2* mutation on cyt $c_6$ *versus* cyt *f* accumulation is interesting because it shows that the role of Ccs1 in the assembly of cyt *f* can be separated from its role in cyt $c_6$ assembly (see also discussion of site-directed mutants, below). Because the mutation occurs within a stromal loop of Ccs1 whereas biochemical evidence clearly places the apocytochrome substrates and site of cytochrome maturation within the lumen, we think it unlikely that the mutation contributes directly to altered interaction with apocytochromes. It is more likely that apocyt *f* is a kinetically favored substrate in the Ccs assembly pathway. A correlation between apoprotein abundance and the molecular lesions in *Ccs1* was not observed in the *Chlamydomonas* mutants. Indeed, the four potentially null mutants (*ccs1-3* through *ccs1-6*) all accumulate apocyt *f* and in some cases to appreciable levels (see apocyt *f* band observed in *ccs1* strains in Fig. 2). The definitive evidence for the proposed chaperone function of Ccs1 therefore requires further study.

Molecular analyses of *ccs1-3*, *ccs1-5*::*NIT1*, and a site-directed C-terminal deletion construct, Δ542–613, highlight the functional importance of the very C-terminal region of the large lumenal domain. Strains *ccs1-3* and *ccs1-5* result from lesions within intron 9. Both strains do accumulate Ccs1 message and retain the potential to encode at least 536 of the 613 amino acids of Ccs1. However, both strains fail to synthesize either holocytochrome $c_6$ or *f* as confirmed by radiolabeling experiments (47), and the C-terminal deletion construct (Δ542–613) fails to rescue *ccs1-4* (data not shown). In all three cases, the truncation in Ccs1 occurs after the third region of sequence conservation (Fig. 5, and see Supplemental Material Figs. 1 and 2), yet the protein is non-functional. In the *B. pertussis* study (49) as well, only the full-length fusion construct was able to complement the *ccsB* mutant. These results emphasize the functional importance of the entire C-terminal domain and argue for the same topological placement of the C terminus on the *p*-side of the membrane where cytochrome maturation occurs.

*A Non-essential Cysteine and Identification of a Functionally Important Histidine*—Site-directed mutagenesis identified a histidinyl residue, His$^{274}$, as important for Ccs1 function in the maturation of *c*-type cytochromes. Two other residues, cysteine 199 and aspartic acid 348 that were absolutely conserved at the start of these studies, were shown by mutagenesis to be non-essential for Ccs1 function. Analysis of 51 Ccs1-like proteins in the data bases (as of May, 2002) revealed that the cysteine residue is totally invariant, but the aspartic acid residue is not conserved. It remains possible that the invariant cysteine residue is important for Ccs1 function but may not be absolutely essential; therefore, the mutation does not present a visible phenotype under the conditions examined. The conserved cysteine is an attractive candidate for participation in the thioreduction pathway involved in cytochrome biogenesis (1, 19). Interestingly, an additional N-terminal domain containing four clustered cysteines, two within a thioredoxin motif, has been identified in the Ccs1 homologue of *B. subtilis*, ResB (83). This cysteine-rich region is present in all *Bacillus* ResB proteins currently identified and in *Geobacillus stearothermophilus* but is lacking in all other identified Ccs1 homologues (data base search May, 2002). The function of this domain remains speculative. Identification and multiple alignments of additional Ccs1 homologues have identified few other conserved residues with attractive functional potential. However, an invariant signature sequence, VN*X*P, located within the large stromal loop (see Fig. 5) that had not been aligned previously (see Ref. 47) has been highlighted. Whether this sequence element could be involved in an interaction with heme is of future research interest.

The H274A mutated version of *Ccs1* is clearly non-functional. The mutated constructs failed to complement *ccs1* mutants regardless of the particular allele used for the transformation experiments, and even when a period of recovery in acetate-supplemented medium was allowed after transformation. Detailed analysis of four strains carrying H274A constructs showed that three of the four strains were completely devoid of holocytochromes in the plastid. The mutations must affect a catalytic function of Ccs1 because the mutated protein does accumulate. A fourth transformant was capable of limited holocyt *f* formation but failed to form holocyt $c_6$, a phenotype that is similar to that of strain *ccs1-2*. We cannot explain why one transformant makes a small amount of holocyt *f*. The four H274A transformants appear to contain comparable amounts of Ccs1, but it is possible that the subtle variations in Ccs1 abundance are not revealed by immunoblot analysis, and it may be that small differences in expression of mutant *Ccs1* genes (resulting from independent integration events in each transformant and accompanying variations in transgene expression (84)) contributes to variations in the severity of the phenotype. We note that all four H274A transformants accumulate very low levels of apocyt *f* but no apocyt $c_6$. Perhaps apocyt $c_6$ is more susceptible to proteolysis relative to apocyt *f* which may be sheltered within the membrane or within the cyt $b_6f$ complex. The presence of a small steady state pool of apocyt *f* but not apocyt $c_6$ may contribute to the preferential synthesis of holocyt *f* in the histidine transformant discussed above and in the *ccs1-2* allele.

In *Wolinella succinogenes*, a protein designated NrfI is responsible for heme attachment to the unique C*XX*CK motif of the pentaheme cytochrome *c* catalytic subunit, NrfA, of nitrite reductase (85). Even though pairwise BLAST analysis (GenBank™) does not reveal significant sequence similarity between any NrfI and any Ccs1, topology predictions based on multiple alignments of NrfI homologues predicts a similar transmembrane structure for the N-terminal two-thirds of NrfI

as for Ccs1. Therefore, NrfI and its homologues may be structurally analogous to a Ccs1/CcsA fusion with three tightly spaced transmembrane domains at the N terminus followed by a large extramembrane domain on the *p*-side, followed by a C-terminal CcsA-related portion containing multiple membrane-spanning segments and a conserved WWD domain. Alignment of NrfI homologues identifies a conserved histidine in the third transmembrane domain, preceding the large soluble domain and positioned toward the *n*-side of the membrane span. We wonder if this histidine is analogous to the essential histidine identified in Ccs1 in this work and indicates a common ancestral origin between NrfI and the CcsA/Ccs1 components in system II.

*Acknowledgments*—We acknowledge the past and present members of the Merchant laboratory for support and intellectual input during the course of this study; J. Leichman and S. Gabilly for technical assistance; Dr. J. Quinn for help during the analysis of *Ccs1* expression; and Dr. J. M. Moseley for generation of the *ccs1-4arg7* strain and for other help during the course of the project. We thank Prof. J.-D. Rochaix, University of Geneva, for hosting B. W. D in his laboratory during which period the *ccs1-6*::*ARG7* strain was identified.

REFERENCES

1. Thöny-Meyer, L. (1997) *Microbiol. Mol. Biol. Rev.* **61,** 337–376
2. Kranz, R., Lill, R., Goldman, B., Bonnard, G., and Merchant, S. (1998) *Mol. Microbiol.* **29,** 383–396
3. Page, M. D., Sambongi, Y., and Ferguson, S. J. (1998) *Trends Biochem. Sci.* **23,** 103–108
4. Xie, Z., and Merchant, S. (1998) *Biochim. Biophys. Acta* **1365,** 309–318
5. Nakamoto, S. S., Hamel, P., and Merchant, S. (2000) *Biochimie* (*Paris*) **82,** 603–614
6. Beckman, D. L., Trawick, D. R., and Kranz, R. G. (1992) *Genes Dev.* **6,** 268–283
7. Goldman, B. S., Beckman, D. L., Bali, A., Monika, E. M., Gabbert, K. K., and Kranz, R. G. (1997) *J. Mol. Biol.* **268,** 724–738
8. Monika, E. M., Goldman, B. S., Beckman, D. L., and Kranz, R. G. (1997) *J. Mol. Biol.* **271,** 679–692
9. Deshmukh, M., Brasseur, G., and Daldal, F. (2000) *Mol. Microbiol.* **35,** 123–138
10. Ramseier, T. M., Winteler, H. V., and Hennecke, H. (1991) *J. Biol. Chem.* **266,** 7793–7803
11. Ritz, D., Bott, M., and Hennecke, H. (1993) *Mol. Microbiol.* **9,** 729–740
12. Ritz, D., Thöny-Meyer, L., and Hennecke, H. (1995) *Mol. Gen. Genet.* **247,** 27–38
13. Page, M. D., and Ferguson, S. J. (1995) *Mol. Microbiol.* **15,** 307–318
14. Page, M. D., Pearce, D. A., Norris, H. A., and Ferguson, S. J. (1997) *Microbiology* **143,** 563–576
15. Page, M. D., and Ferguson, S. J. (1997) *Mol. Microbiol.* **24,** 977–990
16. Page, M. D., and Ferguson, S. J. (1999) *Microbiology* **145,** 3047–3057
17. Thöny-Meyer, L., Fischer, F., Künzler, P., Ritz, D., and Hennecke, H. (1995) *J. Bacteriol.* **17,** 4321–4326
18. Schulz, H., Hennecke, H., and Thöny-Meyer, L. (1998) *Science* **281,** 1197–1200
19. Fabianek, R. A., Hennecke, H., and Thöny-Meyer, L. (2000) *FEMS Microbiol. Rev.* **24,** 303–316
20. Thöny-Meyer, L. (2000) *Biochim. Biophys. Acta* **1459,** 316–324
21. Kranz, R. G. (1989) *J. Bacteriol.* **171,** 456–464
22. Goldman, B. S., Beckman, D. L., Monika, E. M., and Kranz, R. G. (1998) *Proc. Natl. Acad. Sci. U. S. A.* **95,** 5003–5008
23. Goldman, B. S., and Kranz, R. G. (2001) *Res. Microbiol.* **152,** 323–329
24. Beckman, D. L., and Kranz, R. G. (1993) *Proc. Natl. Acad. Sci. U. S. A.* **90,** 2179–2183
25. Vargas, C., Wu, G., Davies, A. E., and Downie, J. A. (1994) *J. Bacteriol.* **176,** 4117–4123
26. Fabianek, R. A., Huber-Wunderlich, M., Glockshuber, R., Künzler, P., Hennecke, H., and Thöny-Meyer, L. (1997) *J. Biol. Chem.* **272,** 4467–4473
27. Page, M. D., Saunders, N. F., and Ferguson, S. J. (1997) *Microbiology* **143,** 3111–3122
28. Fabianek, R. A., Hofer, T., and Thöny-Meyer, L. (1999) *Arch. Microbiol.* **171,** 92–100
29. Reid, E., Cole, J., and Eaves, D. J. (2001) *Biochem. J.* **355,** 51–58
30. Ren, Q., Ahuja, U., and Thöny-Meyer, L. (2002) *J. Biol. Chem.* **277,** 7657–7663
31. Reid, E., Eaves, D. J., and Cole, J. A. (1998) *FEMS Microbiol. Lett.* **166,** 369–375
32. Gaballa, A., Baysse, C., Koedam, N., Muyldermans, S., and Cornelis, P. (1998) *Mol. Microbiol.* **30,** 547–555
33. Schulz, H., Fabianek, R. A., Pellicioli, E. C., Hennecke, H., and Thöny-Meyer, L. (1999) *Proc. Natl. Acad. Sci. U. S. A.* **96,** 6462–6467
34. Ren, Q., and Thöny-Meyer, L. (2001) *J. Biol. Chem.* **276,** 32591–32596
35. Schulz, H., Pellicioli, E. C., and Thöny-Meyer, L. (2000) *Mol. Microbiol.* **37,** 1379–1388
36. Dumont, M. E., Ernst, J. F., Hampsey, D. M., and Sherman, F. (1987) *EMBO J.* **6,** 235–241
37. Drygas, M. E., Lambowitz, A. M., and Nargang, F. E. (1989) *J. Biol. Chem.* **264,** 17897–17906
38. Zollner, A., Rodel, G., and Haid, A. (1992) *Eur. J. Biochem.* **207,** 1093–1100
39. Cervera, A. M., Gozalbo, D., McCreath, K. J., Gow, N. A., Martinez, J. P., and Casanova, M. (1998) *Mol. Microbiol.* **30,** 67–81
40. Steiner, H., Zollner, A., Haid, A., Neupert, W., and Lill, R. (1995) *J. Biol. Chem.* **270,** 22842–22849
41. Zhang, L., and Guarente, L. (1995) *EMBO J.* **14,** 313–320
42. Kranz, R. G., Beckett, C. S., and Goldman, B. S. (2002) *Res. Microbiol.* **153,** 1–6
43. Howe, G., and Merchant, S. (1992) *EMBO J.* **11,** 2789–2801
44. Xie, Z., Culler, D., Dreyfuss, B. W., Kuras, R., Wollman, F. A., Girard-Bascou, J., and Merchant, S. (1998) *Genetics* **148,** 681–692
45. Dreyfuss, B. W., and Merchant, S. (1998) in *Photosynthesis: Mechanisms and Effects* (Garab, G., ed) Vol. IV, pp. 3139–3142, Kluwer Academic Publishers, The Netherlands
46. Xie, Z., and Merchant, S. (1996) *J. Biol. Chem.* **271,** 4632–4639
47. Inoue, K., Dreyfuss, B. W., Kindle, K. L., Stern, D. B., Merchant, S., and Sodeinde, O. A. (1997) *J. Biol. Chem.* **272,** 31747–31754
48. Schiött, T., Throne-Holst, M., and Hederstedt, L. (1997) *J. Bacteriol.* **179,** 4523–4529
49. Beckett, C. S., Loughman, J. A., Karberg, K. A., Donato, G. M., Goldman, W. E., and Kranz, R. G. (2000) *Mol. Microbiol.* **38,** 465–481
50. Lennartz, K., Plücken, H., Seidler, A., Westhoff, P., Bechtold, N., and Meierhoff, K. (2001) *Plant Cell* **13,** 2539–2551
51. Sun, G., Sharkova, E., Chesnut, R., Birkey, S., Duggan, M. F., Sorokin, A., Pujic, P., Ehrlich, S. D., and Hulett, F. M. (1996) *J. Bacteriol.* **178,** 1374–1385
52. Schiött, T., von Wachenfeldt, C., and Hederstedt, L. (1997) *J. Bacteriol.* **179,** 1962–1973
53. Katzen, F., Deshmukh, M., Daldal, F., and Beckwith, J. (2002) *EMBO J.* **21,** 3960–3969
54. Tichy, M., and Vermaas, W. (1999) *J. Biol. Chem.* **274,** 32396–32401
55. Hamel, P., Dreyfuss, B. W., Xie, Z., Gabilly, S., and Merchant, S. (2002) *J. Biol. Chem.* **277,** 2593–2603
56. Gorman, D. S., and Levine, R. P. (1966) *Plant Physiol.* **41,** 1648–1656
57. Lemaire, C., Girard-Bascou, J., Wollman, F.-A., and Bennoun, P. (1986) *Biochim. Biophys. Acta* **851,** 229–238
58. Harris, E. H. (1989) *The Chlamydomonas Sourcebook: A Comprehensive Guide to Biology and Laboratory Use*, Academic Press, San Diego
59. Gumpel, N. J., Rochaix, J. D., and Purton, S. (1994) *Curr. Genet.* **26,** 438–442
60. Kindle, K. L. (1990) *Proc. Natl. Acad. Sci. U. S. A.* **87,** 1228–1232
61. Fenton, J. M., and Crofts, A. R. (1990) *Photosynth. Res.* **26,** 59–66
62. Funke, R., Kovar, J., and Weeks, D. P. (1997) *Plant Physiol.* **114,** 237–244
63. Lumbreras, V., Stevens, D. R., and Purton, S. (1998) *Plant J.* **14,** 441–447
64. Quinn, J. M., Nakamoto, S. S., and Merchant, S. (1999) *J. Biol. Chem.* **274,** 14444–14454
65. Li, H. H., Quinn, J., Culler, D., Girard-Bascou, J., and Merchant, S. (1996) *J. Biol. Chem.* **271,** 31283–31289
66. Chen, X., Kindle, K. L., and Stern, D. B. (1995) *Plant Cell* **7,** 1295–1305
67. Church, G., and Gilbert, W. (1984) *Proc. Natl. Acad. Sci. U. S. A.* **81,** 1991–1995
68. Merchant, S., Hill, K., Kim, J. H., Thompson, J., Zaitlin, D., and Bogorad, L. (1990) *J. Biol. Chem.* **265,** 12372–12379
69. Tautz, D., and Renz, M. (1983) *Anal. Biochem.* **132,** 14–19
70. Merchant, S., and Bogorad, L. (1986) *Mol. Cell. Biol.* **6,** 462–469
71. Ho, S., Hunt, D., Horton, R., Pullen, J., and Pease, L. (1989) *Gene* (*Amst.*) **77,** 51–59
72. Hill, K. L., and Merchant, S. (1995) *EMBO J.* **14,** 857–865
73. Cahoon, A. B., and Timko, M. P. (2000) *Plant Cell* **12,** 559–568
74. Ohad, I. (1974) *Methods Enzymol.* **32,** 865–871
75. Malnoe, P., Mayfield, S. P., and Rochaix, J. D. (1988) *J. Cell Biol.* **106,** 609–616
76. Schuster, G., Neuchushtai, R., Ferreira, P. C., Thornber, J. P., and Ohad, I. (1988) *Eur. J. Biochem.* **177,** 411–416
77. Anderson, C. M., and Gray, J. C. (1991) *Plant Physiol.* **96,** 584–587
78. Schuldiner, S., and Ohad, I. (1969) *Biochim. Biophys. Acta* **180,** 165–177
79. de Heij, H. T., Jochemsen, A. G., Willemsen, P. T., and Groot, G. S. (1984) *Eur. J. Biochem.* **138,** 161–168
80. Kuras, R., and Wollman, F.-A. (1994) *EMBO J.* **13,** 1019–1027
81. Rost, B., Casadio, R., Fariselli, P., and Sander, C. (1995) *Protein Sci.* **4,** 521–533
82. Maquat, L. E. (2002) *Science* **295,** 2221–2222
83. Le Brun, N. E., Bengtsson, J., and Hederstedt, L. (2000) *Mol. Microbiol.* **36,** 638–650
84. Harris, E. H. (2001) *Annu. Rev. Plant Physiol. Plant Mol. Biol.* **52,** 363–406
85. Pisa, R., Stein, T., Eichler, R., Gross, R., and Simon, J. (2002) *Mol. Microbiol.* **43,** 763–770
86. Auchincloss, A. H., Loroch, A. I., and Rochaix, J. D. (1999) *Mol. Gen. Genet.* **261,** 21–30
87. Quinn, J. M., and Merchant, S. (1998) *Methods Enzymol.* **297,** 263–279
88. von Heijne, G. (1992) *J. Mol. Biol.* **225,** 487–494

**SUPPLEMENTAL EXPERIMENTAL PROCEDURES**

***Generation of Ccs1 antiserum ¾*** The 1625-base pair cDNA fragment corresponding to amino acid residues 303-506 was amplified from the *Ccs1* cDNA clone (Inoue et al., 1997, *J. Biol. Chem.* **272**, 31747) using primers TRX5' and TRX3', cloned in-frame into the tryptophan-inducible expression vector pTrxFus (Invitrogen Corp., San Diego, CA), and introduced into *E. coli* strain GI274. Cells were grown in RM medium (42 mM $Na_2PO_4$, 17 mM $KH_2PO_4$, 8.5 mM NaCl, 18 mM $NH_4Cl$, 1 mM MgCl, 20 µg/ml casamino acids) with 100 µg/mL ampicillin. Expression was maximized by optimization of growth conditions. The fusion protein localized to inclusion bodies, which were visible under 100X magnification. Cutures were centrifuged at 9,820 x *g* for 10 min at 4°C and the resulting pellet was resuspended in (1/10 culture volume) TGE (25 mM TrisHCl (pH 8.0), 10 mM EDTA, 50 mM glucose). Cells were lysed by sonication (3 x 30 sec; probe sonicator at 35% - 0.6 relative output) and freeze-thaw cycles. Inclusion bodies were prepared by washing in TGE with 1% Triton X-100 (1/50 culture volume), and centrifuging at 7,740 x *g* for 10 min at 4 °C. An enriched inclusion body sample was solubilized in 7M urea, 50mM Tris (pH 8.3), 20mM NaCl, 2mM DTT at 4 °C overnight followed by dialysis. Polyclonal antibodies were raised in Elite rabbits by Covance Research Products Inc. (Denver, PA) by popliteal lymph node injection (200 µg antigen), followed by intranodal boosts (2 x 250 µg antigen, 1 x 200 µg antigen). The antiserum recognizes a protein of approximately 60kDa that is present in wild-type samples and absent in *ccs1* mutants.

***Preparation of nucleic acid ¾*** For isolation of total genomic DNA, cells were harvested by centrifugation (4,400 x *g*, 5 min), resuspended in lysis buffer (10 mM Tris (pH8.0), 10 mM EDTA, 10 mM NaCl; 0.5% SDS; 200 µg/ml proteinase K) and incubated at 50 °C for 2 hours.

Cell lysate was extracted with phenol/$CHCl_3$. The aqueous phase was treated with RNaseA (20 µg/ml) at 37 °C for 30 min and then extracted once more with phenol/$CHCl_3$. CsCl was dissolved in the aqueous phase to yield ≈ 83% solution and ethidium bromide was added from a 10 mg/ml stock to 0.2 µg/ml final concentration. The CsCl gradients were centrifuged in an NVT65 rotor (Beckman) at 65,000 rpm, 15 °C, overnight. Genomic DNA bands were removed from gradients, dialyzed against three successive solutions of 50 mM Tris (pH8.0), 10 mM EDTA, 0.5 M NaCl; followed by 50 mM Tris (pH 8.0), 10 mM EDTA, and finally 10 mM Tris (pH 8.0), 10 mM EDTA. Nucleic acids were precipitated in ethanol (70%) and resuspended in 10 mM Tris (pH 8.0), 10 mM EDTA.

***Constructions of CcsB-PhoA and CcsB-LacZ fusions ¾*** Whole genomic DNA from *Synechocystis* sp. PCC 6803 strain (a generous gift from X. Zhou and P. Chitnis) was used as a template along with F-ccsBSac as a forward primer and a fusion specific R-ccsB oligonucleotide as a reverse primer (see primers in Supplemental Table II). F-Ccs1Sac was engineered with a *Sac*I site upstream of the first ATG codon in the *ccsB* ORF (Tichy and Vermass, 1999, *J. Biol. Chem.* **274**, 32396) and R-ccsB primers were designed with a *Sal*I site at the desired CcsB-PhoA fusion junction. PCR products were digested with *Sac*I and *Sal*I and cloned into *Sac*I/*Sal*I digested pRGK200 (Monika et al., 1997, *J. Mol. Biol*. **271**, 679), in frame with the downstream *phoA* gene encoding alkaline phosphatase. The fusions at positions 288, 349, 416, 458 of the CcsB polypeptide were engineered in plasmid p*ccsB-225:phoA.* PCR fragments were amplified from *Synechocystis* genomic DNA using F-ccsBNde as a forward primer and the R-ccsB reverse primer corresponding to the desired site of the translational fusion. Primer F-ccsBNde spans a *Nde*I site that is unique in *ccsB* ORF and corresponds to position 199-200 of the CcsB polypeptide. The *Nde*I/*Sal*I fragment from p*ccsB-225:phoA* was replaced by the *Nde*I/*Sal*I

digested PCR products. The resulting plasmids express translational fusions of CcsB to PhoA at positions 288, 349, 416 and 458.

***Generation of site-directed mutant strains ¾*** Complementary mutagenic primer C199A-1 and C199A-2, H274A-1 and H274A-2, and D348A-1 and D348A-2 and gene specific primers flanking restriction sites utilized subsequently for subcloning were used to amplify fragments from p*Ccs1* in all first round amplifications. Products from the first round of amplification were gel purified using the QiaEx II gel extraction protocol (QIAGEN Inc., Valencia, CA) and served as templates for the second round. For C199A, primers CCS1-13 and C199A-2 as well as CCS1-14 and C199A-1 were used in the first round of amplification followed by a second round of amplification using CCS1-13 and CCS1-14 to amplify a 528-base pair fragment containing *Bsa*I and *Eco47*III sites for subcloning. For H274A, primers CCS1-5 and H274A-2 as well as CCS1-8 and H274A-1 were used in the first round of amplification followed by a second round of amplification using primers CCS1-5 and CCS1-8 to amplify a 503-base pair fragment containing *BsiW*I and *Msc*I sites for subcloning. For both C199A and H274A, the PCR conditions were 30 cycles of 95 °C for 45 seconds, 55 °C for 45 seconds, 72 °C for 1.5 minutes. For D348A, primers D348A-1 and CCS1-18 as well as D348A-2 and H274A-1 were used in the first round of amplification followed by a second amplification using primers CCS1-18 and H274A-1 to amplify a 1.6 kb fragment containing *Msc*I and *Sgr*AI sites for subcloning. PCR conditions were 30 cycles of 95 °C for 45 seconds, 58 °C for 45 seconds, 72 °C for 2 minutes.

Supplemental Figure 1.

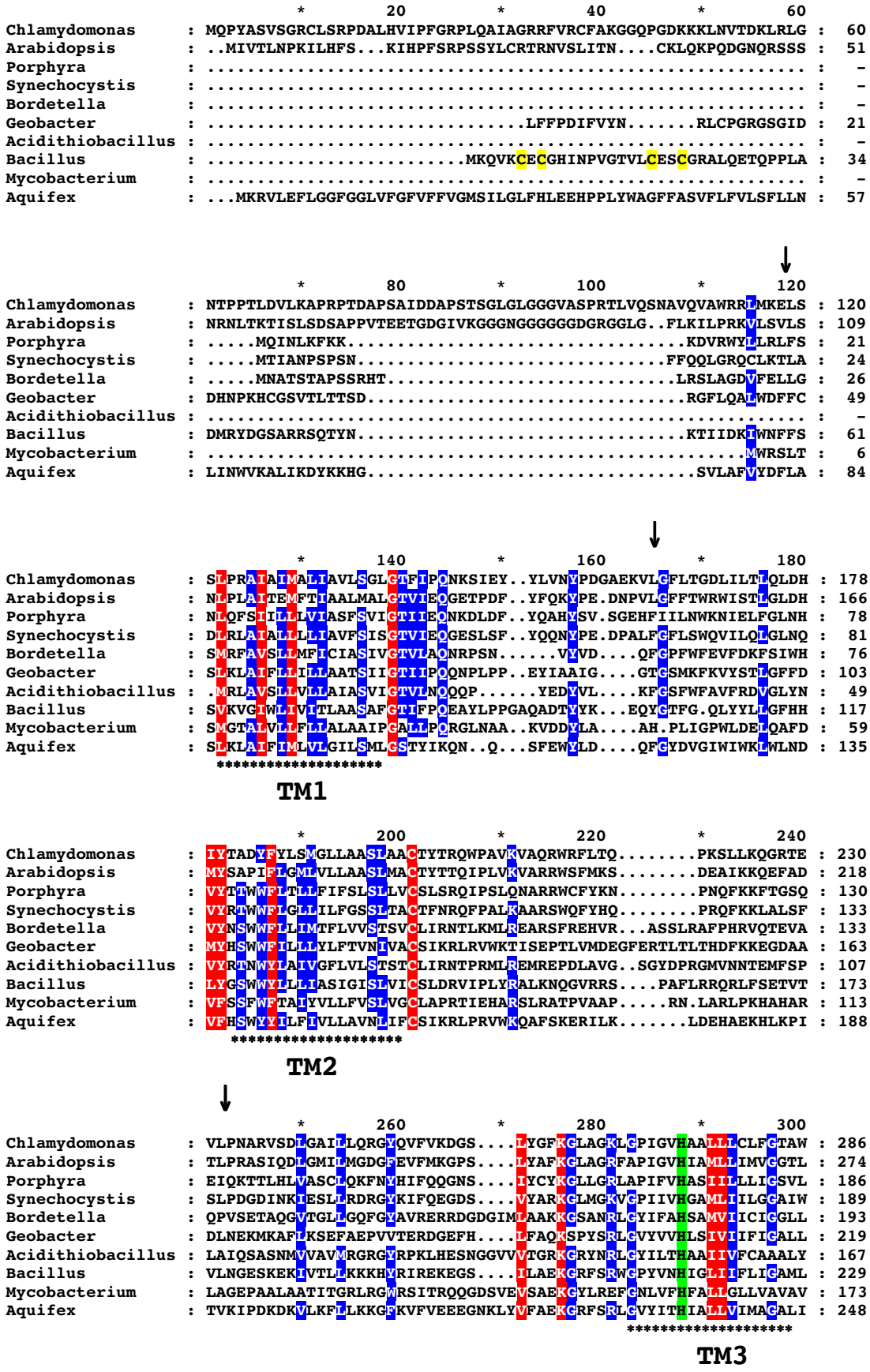

Supplemental Fig. 1, Dreyfuss et al.

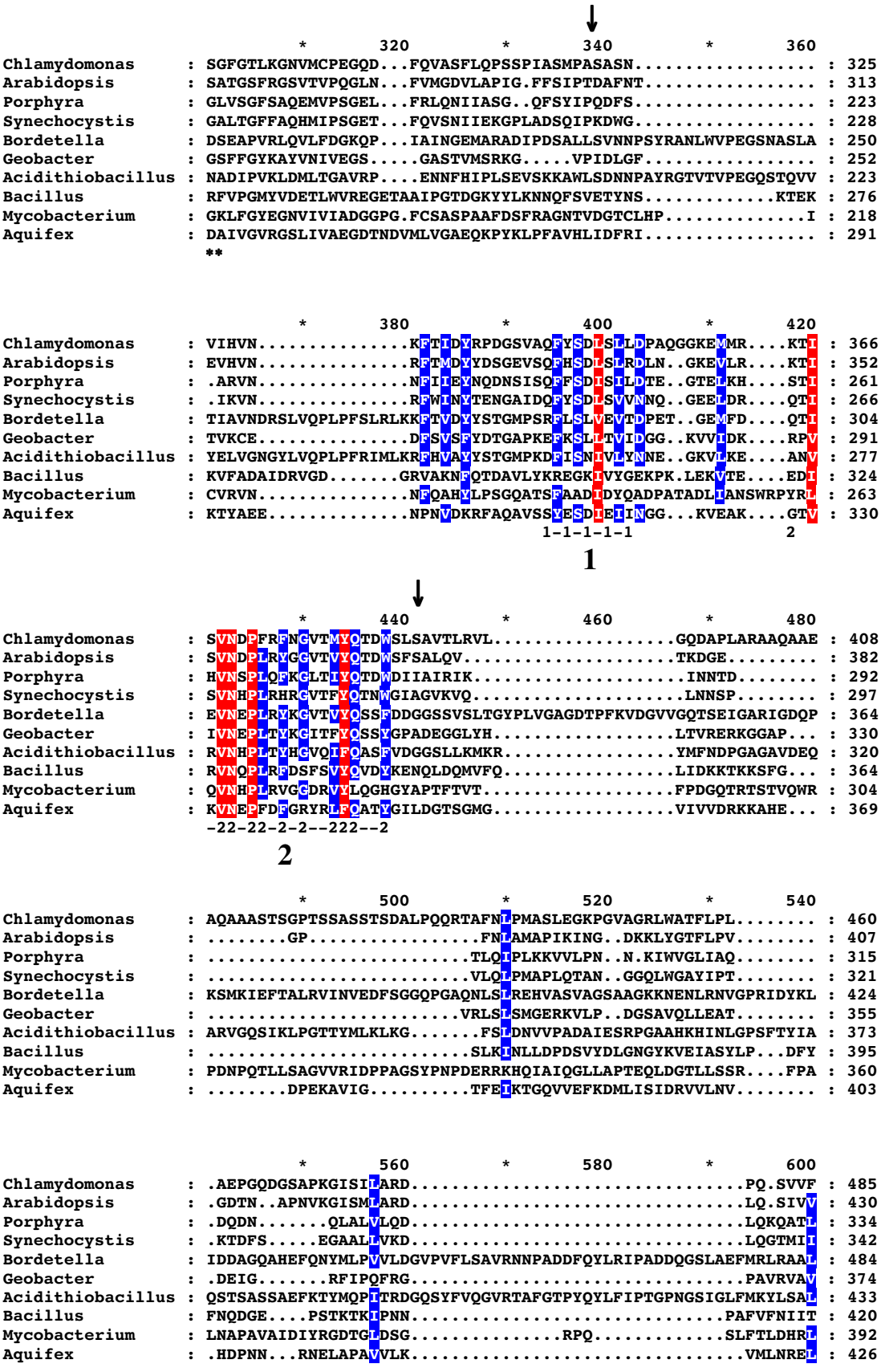

Supplemental Fig. 1, Dreyfuss et al.

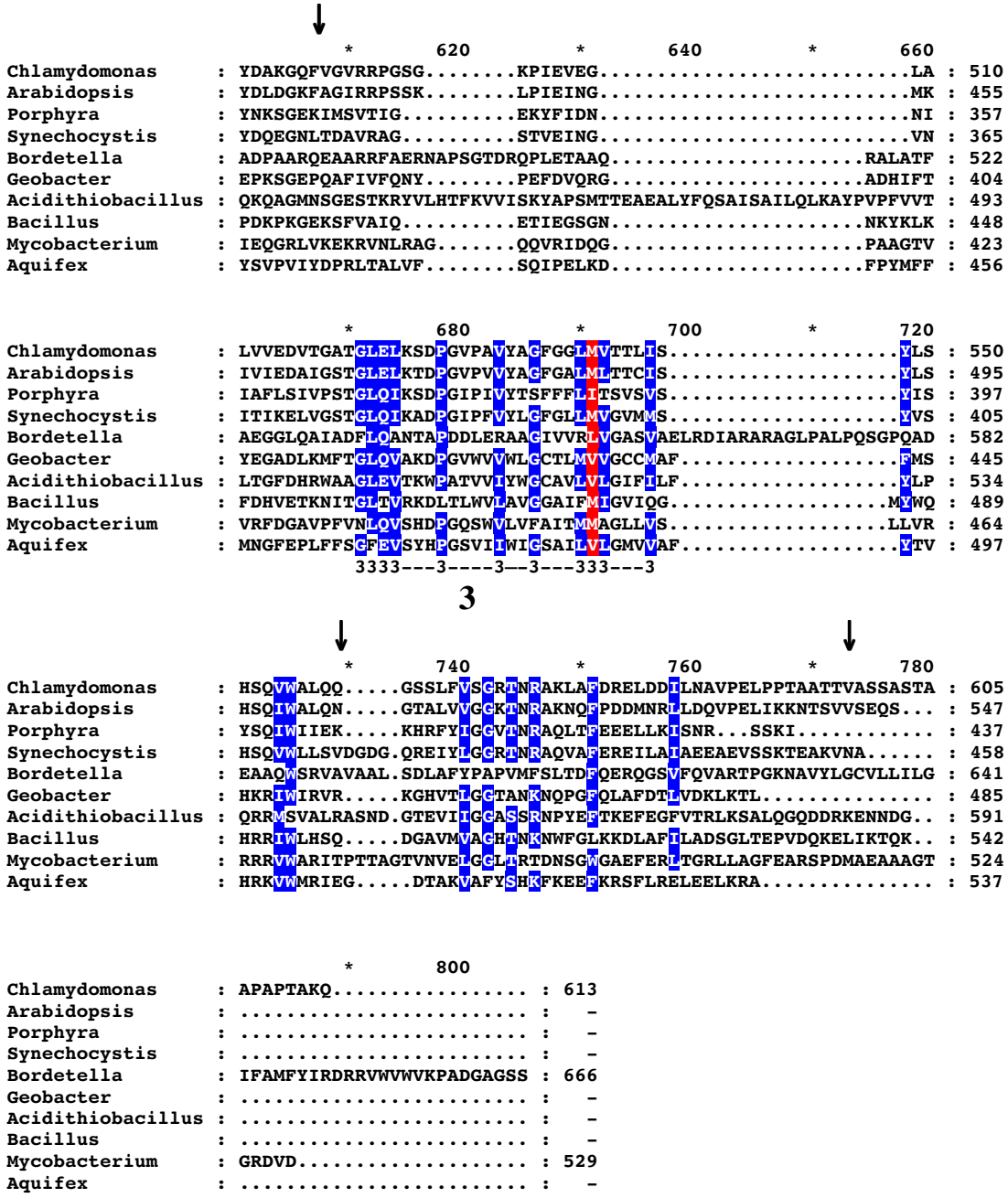

Supplemental Figure 2.

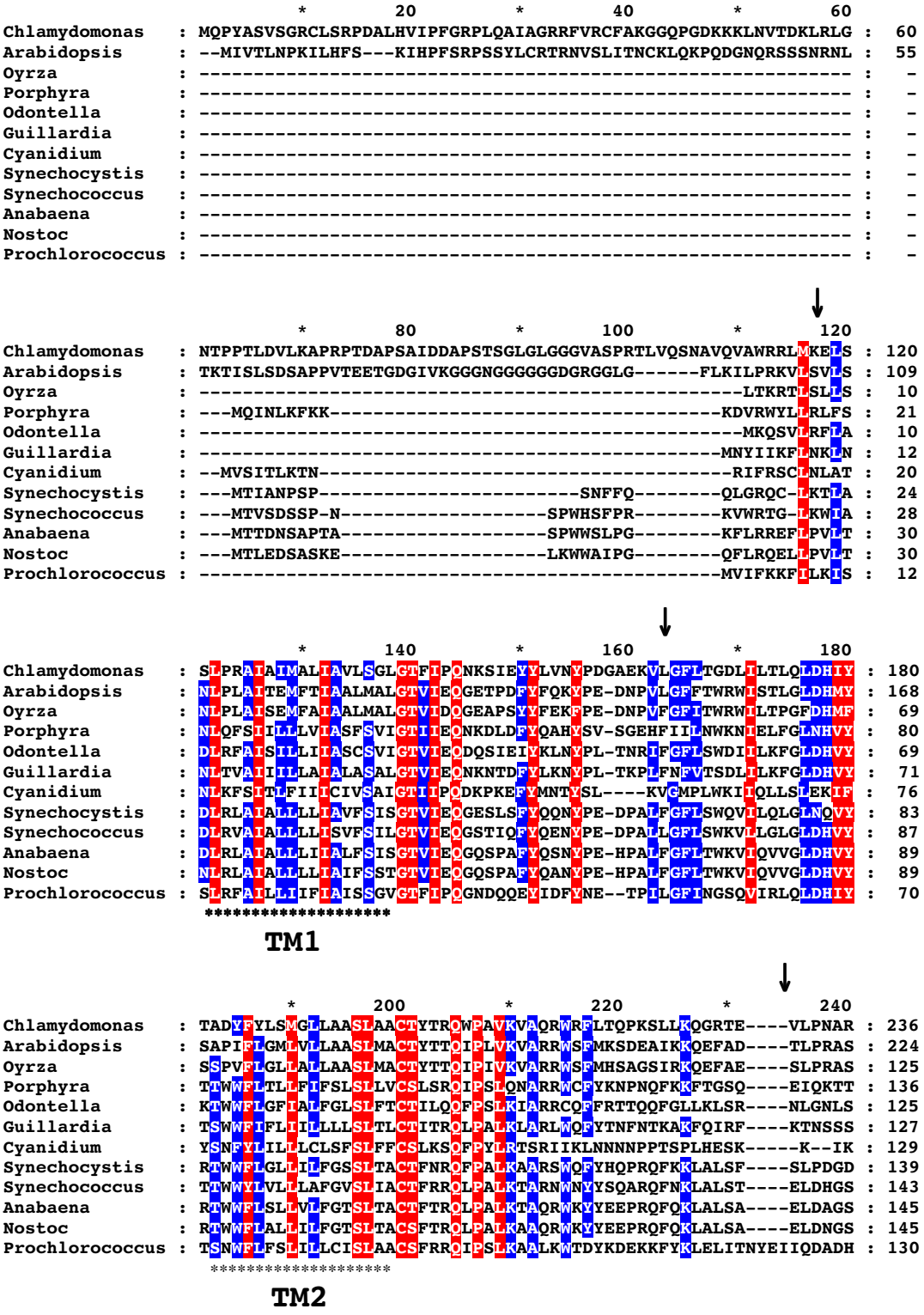

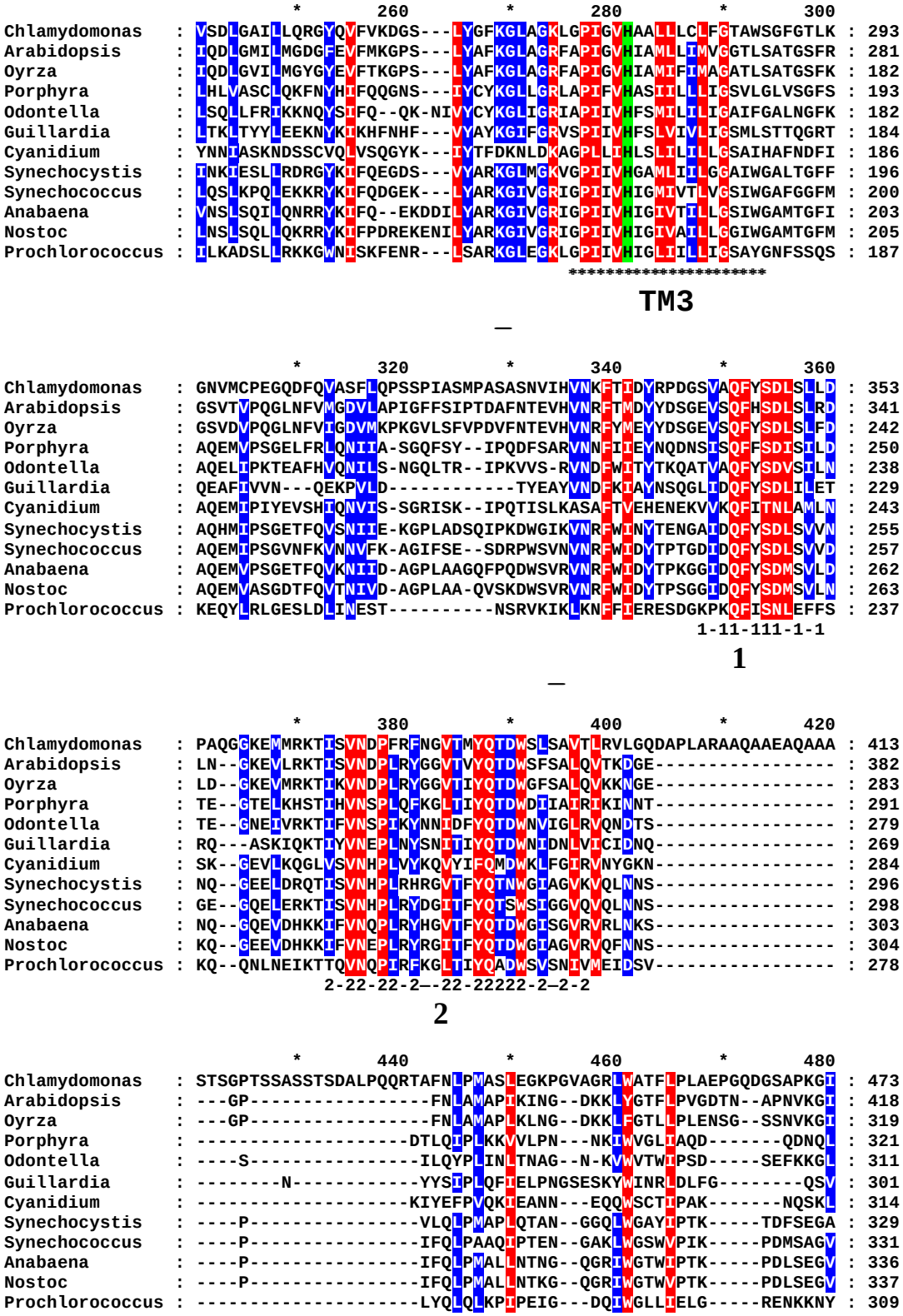
260
280
300
Chlamydomonas : VSDLGAILQRGYQVFVKDGS---LYGFKGLAGKLGPIGVHAALLCLFGTAWSGFGTLK : 293
Arabidopsis : IQDLGMILMGDGFEVFMKGPS---LYAFKGLAGRFAPIGVHIAMLLIMVGGTLSATGSFR : 281
Oyrza : IQDLGVILMGYGYEVFTKGPS---LYAFKGLAGRFAPIGVHIAMIFIMAGATLSATGSFK : 182
Porphyra : LHLVASCLQKFNYHIFQQGNS---IYCYKGLLGRLAPIFVHASIILLLIGSVLGLVSGFS : 193
Odontella : LSQLLFRIKKNQYSIFQ--QK-NIVYCYKGLIGRIAPIIVHFSMILILIGAIFGALNGFK : 182
Guillardia : LTKLTYYLEEKNYKIKHFNHF---VYAYKGIFGRVSPIIVHFSLVIVLIGSMLSTTQGRT : 184
Cyanidium : YNNIASKNDSSCVQLVSQGYK---IYTFDKNLDKAGPLLIHLSLILILLGSAIHAFNDFI : 186
Synechocystis : INKIESLLRDRGYKIFQEGDS---VYARKGLMGKVGPIIVHGAMLIILGGAIWGALTGFF : 196
Synechococcus : LQSLKPQLEKKRYKIFQDGEK---LYARKGIVGRIGPIIVHIGMIVTLVGSIWGAFGGFM : 200
Anabaena : VNSLSQILQNRRYKIFQ--EKDDILYARKGIVGRIGPIIVHIGIVTILLGSIWGAMTGFI : 203
Nostoc : LNSLSQLLQKRRYKIFPDREKENILYARKGIVGRIGPIIVHIGIVAILLGGIWGAMTGFM : 205
Prochlorococcus : ILKADSLLRKKGWNISKFENR---LSARKGLEGKLGPIIVHIGLIILLIGSAYGNFSSQS : 187
**********
TM3
320
340
360
Chlamydomonas : GNVMCPEGQDFQVASFLQPSSPIASMPASASNVIHVNKFTIDYRPDGSVAQFYSDLSLLD : 353
Arabidopsis : GSVTVPQGLNFVMGDVLAPIGFFSIPTDAFNTEVHVNRFTMDYYDSGEVSQFHSDLSLRD : 341
Oyrza : GSVDVPQGLNFVIGDVMKPKGVLSFVPDVFNTEVHVNRFYMEYYDSGEVSQFYSDLSLFD : 242
Porphyra : AQEMVPSGELFRLQNIIA-SGQFSY--IPQDFSARVNNFIIEYNQDNSISQFFSDISILD : 250
Odontella : AQELIPKTEAFHVQNILS-NGQLTR--IPKVVS-RVNDFWITYTKQATVAQFYSDVSILN : 238
Guillardia : QEAFIVVN---QEKPVLD-----------TYEAYVNDFKIAYNSQGLIDQFYSDLILET : 229
Cyanidium : AQEMIPIYEVSHIQNVIS-SGRISK--IPQTISLKASAFTVEHENEKVVKQFITNLAMLN : 243
Synechocystis : AQHMIPSGETFQVSNIIE-KGPLADSQIPKDWGIKVNRFWINYTENGAIDQFYSDLSVVN : 255
Synechococcus : AQEMIPSGVNFKVNNVFK-AGIFSE--SDRPWSVNVNRFWIDYTPTGDIDQFYSDLSVVD : 257
Anabaena : AQEMVPSGETFQVKNIID-AGPLAAGQFPQDWSVRVNRFWIDYTPKGGIDQFYSDMSVLD : 262
Nostoc : AQEMVASGDTFQVTNIVD-AGPLAA-QVSKDWSVRVNRFWIDYTPSGGIDQFYSDMSVLN : 263
Prochlorococcus : KEQYLRLGESLDLINEST----------NSRVKIKLKNFFIERESDGKPKQFISNLEFFS : 237
1-11-111-1-1
1
380
400
420
Chlamydomonas : PAQGGKEVMRKTISVNDPFRGNGVTMYQTDWSLSAVTLRVLGQDAPLARAAQAAEAQAAA : 413
Arabidopsis : LN--GKEVLRKTISVNDPLRYGGVTVYQTDWSFSALQVTKDGE---------------- : 382
Oyrza : LD--GKEVMRKTIKVNDPLRYGGVTIYQTDWGFSALQVKKNGE---------------- : 283
Porphyra : TE--GTELKHSTIHVNSPLQFKGLTIYQTDWDIIAIRIKINNT---------------- : 291
Odontella : TE--GNEIVRKTIFVNSPIKYNNIDFYQTDWNVIGLRVQNDTS---------------- : 279
Guillardia : RQ---ASKIQKTIYVNEPLNYSNITIYQTDWNIDNLVICIDNQ---------------- : 269
Cyanidium : SK--GEVLKQGLVSVNHPLVYKQVYIFQMDWKLFGIRVNYGKN---------------- : 284
Synechocystis : NQ--GEELDRQTISVNHPLRHRGVTFYQTNWGIAGVKVQLNNS---------------- : 296
Synechococcus : GE--GQELERKTISVNHPLRYDGITFYQTSWSIGGVQVQLNNS---------------- : 298
Anabaena : NQ--GQEVDHKKIFVNQPLRYHGVTFYQTDWGISGVRVRLNKS---------------- : 303
Nostoc : KQ--GEEVDHKKIFVNEPLRYRGITFYQTDWGIAGVRVQFNNS---------------- : 304
Prochlorococcus : KQ--QNLNEIKTTQVNQPIRFKGLTIYQADWSVSNIVMEIDSV---------------- : 278
2-22-22-2—-22-22222-2—2-2
2
440
460
480
Chlamydomonas : STSGPTSSASSTSDALPQQRTAFNLPMASLEGKPGVAGRLWATFLPLAEPGQDGSAPKGI : 473
Arabidopsis : ---GP----------------FNLAMAPIKING--DKKLYGTFLPVGDTN--APNVKGI : 418
Oyrza : ---GP----------------FNLAMAPLKLNG--DKKLFGTLLPLENSG--SSNVKGI : 319
Porphyra : -------------------DTLQIPLKKVVLPN---NKIWVGLIAQD-------QDNQL : 321
Odontella : ----S---------------ILQYPLINLTNAG--N-KVWVTWIPSD-----SEFKKGL : 311
Guillardia : --------N-----------YYSIPLQFIELPNGSESKYWINRLDLFG--------QSV : 301
Cyanidium : -------------------KIYEFPVQKIEANN---EQQWSCTIPAK-------NQSKL : 314
Synechocystis : ----P---------------VLQLPMAPLQTAN--GGQLWGAYIPTK-----TDFSEGA : 329
Synechococcus : ----P---------------IFQLPAAQIPTEN--GAKLWGSWVPIK-----PDMSAGV : 331
Anabaena : ----P---------------IFQLPMALLNTNG--QGRIWGTWIPTK-----PDLSEGV : 336
Nostoc : ----P---------------IFQLPMALLNTKG--QGRIWGTWVPTK-----PDLSEGV : 337
Prochlorococcus : -------------------LYQLQLKPIPEIG---DQIWGLLIELG-----RENKKNY : 309

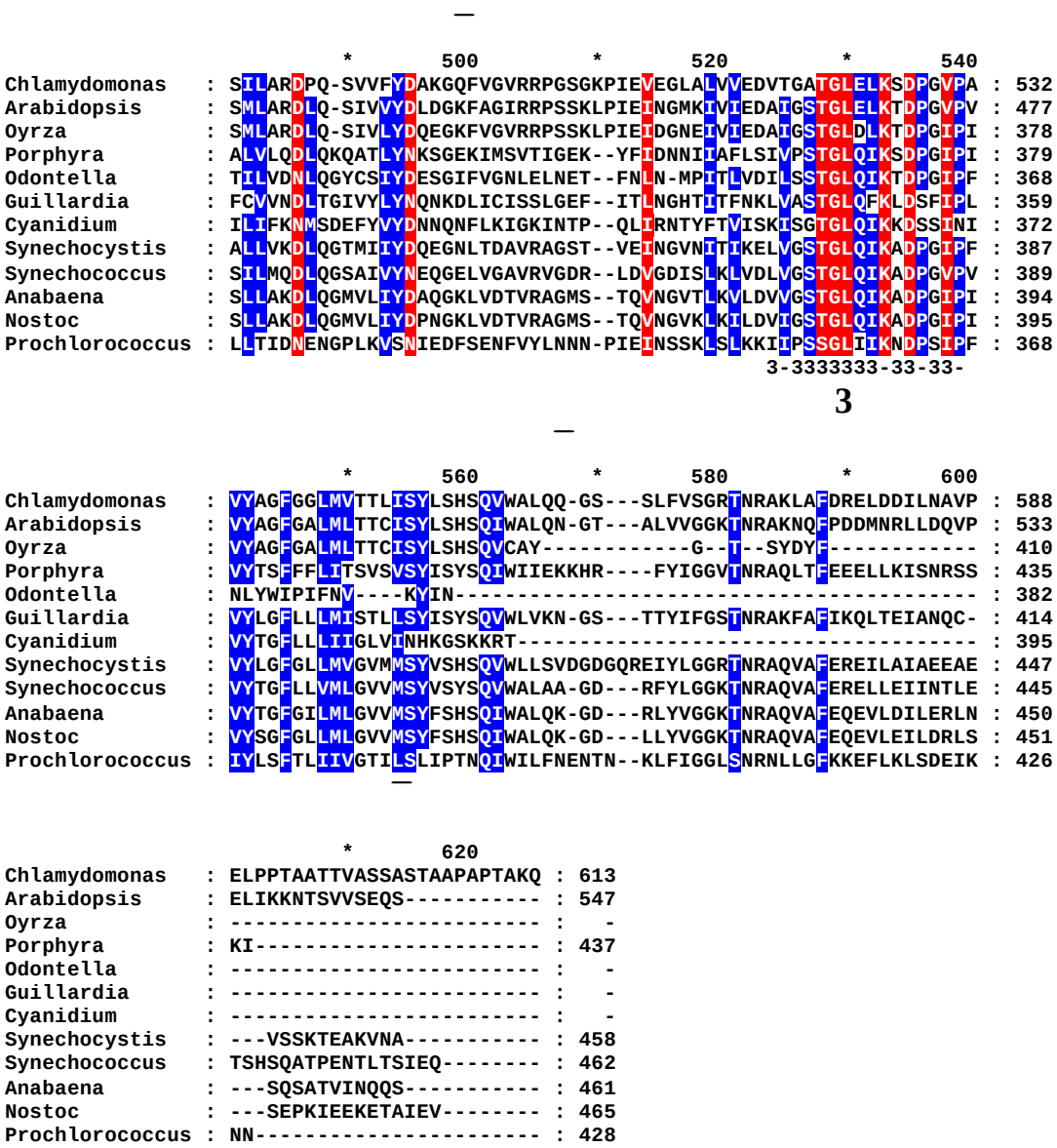
500
520
540
Chlamydomonas : SILARDPQ-SVVFYDAKGQFVGVRRPGSGKPIEVEGLALVVEDVTGATGLELKSDPGVPA : 532
Arabidopsis : SMLARDLQ-SIVVYDLDGKFAGIRRPSSKLPIEINGMKIVIEDAIGSTGLELKTDPGVPV : 477
Oyrza : SMLARDLQ-SIVLYDQEGKFVGVRRPSSKLPIEIDGNEIVIEDAIGSTGLDLKTDPGIPI : 378
Porphyra : ALVLQDLQKQATLYNKSGEKIMSVTIGEK--YFIDNNIIAFLSIVPSTGLQIKSDPGIPI : 379
Odontella : TILVDNLQGYCSIYDESGIFVGNLELNET--FNLN-MPITLVDILSSTGLQIKTDPGIPF : 368
Guillardia : FCVVNDLTGIVYLYNQNKDLICISSLGEF--ITLNGHTITFNKLVASTGLQFKLDSFIPL : 359
Cyanidium : ILIFKNMSDEFYVYDNNQNFLKIGKINTP--QLIRNTYFTVISKISGTGLQIKKDSSINI : 372
Synechocystis : ALLVKDLQGTMIIYDQEGNLTDAVRAGST--VEINGVNITIKELVGSTGLQIKADPGIPF : 387
Synechococcus : SILMQDLQGSAIVYNEQGELVGAVRVGDR--LDVGDISLKLVDLVGSTGLQIKADPGVPV : 389
Anabaena : SLLAKDLQGMVLIYDAQGKLVDTVRAGMS--TQVNGVTLKVLDVVGSTGLQIKADPGIPI : 394
Nostoc : SLLAKDLQGMVLIYDPNGKLVDTVRAGMS--TQVNGVKLKILDVIGSTGLQIKADPGIPI : 395
Prochlorococcus : LLTIDNENGPLKVSNIEDFSENFVYLNNN-PIEINSSKLSLKKIIPSSGLIIKNDPSIPF : 368
3-3333333-33-33-
3
560
580
600
Chlamydomonas : VYAGFGGLMVTTLISYLSHSQVWALQQ-GS---SLFVSGRTNRAKLAFDRELDDILNAVP : 588
Arabidopsis : VYAGFGALMLTTCISYLSHSQIWALQN-GT---ALVVGGKTNRAKNQFPDDMNRLLDQVP : 533
Oyrza : VYAGFGALMLTTCISYLSHSQVCAY----------G--T--SYDYF---------- : 410
Porphyra : VYTSFFFLITSVSVSYISYSQIWIIEKKHR----FYIGGVTNRAQLTFEEELLKISNRSS : 435
Odontella : NLYWIPIFNV----KYIN---------- : 382
Guillardia : VYLGFLLLMISTLLSYISYSQVWLVKN-GS---TTYIFGSTNRAKFAFIKQLTEIANQC- : 414
Cyanidium : VYTGFLLLIIGLVINHKGSKKRT---------- : 395
Synechocystis : VYLGFGLLMVGVMMSYVSHSQVWLLSVDGDGQREIYLGGRTNRAQVAFEREILAIAEEAE : 447
Synechococcus : VYTGFLLVMLGVVMSYVSYSQVWALAA-GD---RFYLGGKTNRAQVAFERELLEIINTLE : 445
Anabaena : VYTGFGILMLGVVMSYFSHSQIWALQK-GD---RLYVGGKTNRAQVAFEQEVLDILERLN : 450
Nostoc : VYSGFGLLMLGVVMSYFSHSQIWALQK-GD---LLYVGGKTNRAQVAFEQEVLEILDRLS : 451
Prochlorococcus : IYLSFTLIIVGTILSLIPTNQIWILFNENTN--KLFIGGLSNRNLLGFKKEFLKLSDEIK : 426
620
Chlamydomonas : ELPPTAATTVASSASTAAPAPTAKQ : 613
Arabidopsis : ELIKKNTSVVSEQS---------- : 547
Oyrza : ---------- : -
Porphyra : KI---------- : 437
Odontella : ---------- : -
Guillardia : ---------- : -
Cyanidium : ---------- : -
Synechocystis : ---VSSKTEAKVNA---------- : 458
Synechococcus : TSHSQATPENTLTSIEQ-------- : 462
Anabaena : ---SQSATVINQQS---------- : 461
Nostoc : ---SEPKIEEKETAIEV-------- : 465
Prochlorococcus : NN---------- : 428

Supplemental Figure. 1. **Multiple alignment of Ccs1 from phyllogenetic representative organisms**.

Ccs1 homologs from green algae *Chlamydomonas reinhardtii* (T09105), eudicot plant *Arabidopsis thaliana* (NC_003070), plastid genome of red algae *Porphyra purpurea* (NC_000925), cyanobacterial *Synechocystis* sp. PCC 6803 (NC_000911), beta-proteobacterium *Bordetella pertussis* (Sanger 520, complete genome), delta-proteobacterium *Geobacter sulfurreducens* (TIGR_35554, preliminary sequence data was obtained from The Institute for Genomic research website at http://www.tigr.org, ORF predicted to initiate at UUG start codon), gamma-proteobacterium *Acidithiobacillus ferrooxidans* (AAC68692), Bacillus group of Firmicutes bacterium *Bacillus subtilis* (NC_000964), Actinobactium group of Firmicutes bacterium *Mycobacterium tuberculosis* CDC1551(NP_334959), and Aquificales bacterium *Aquiflex aeolicus* (NC_000918) were aligned using CLUSTALW algorithm (Blosum62 scoring matrix) in Bioedit software (http://www.mbio.ncsu.edu/BioEdit/bioedit.html). The alignment was edited in the GeneDoc multiple alignment editor software (http://www.psc.edu/biomed/genedoc/). Amino-acids conserved in all sequences are shaded red and those conserved in the majority of the sequences are shaded blue. Location of transmembrane (TM) domains predicted by PHD algorithm (http://www.embl-heidelberg.de/predictprotein/predictprotein.html) are underlined (*). Sites of *phoA* and *LacZ* fusions constructs are marked with arrows above sequences. Functionally essential histidine (H274 in *C. reinhardtii*) is highlighted in green. Three blocks of conserved sequences in the predicted soluble lumenal domain are marked below the sequences as with 1, 2 and 3 respectively.

Supplemental Figure. 2. **Multiple alignment of Ccs1 from representative oxygenic photosynthetic organisms.**

Ccs1 homologs from the nuclear genome of green algae *Chlamydomonas reinhardtii* (T09105), eudicot plant *Arabidopsis thaliana* (NC_003070), monocot *Oryza sativa* (hypothetical protein), plastid genome of red algae *Porphyra purpurea* (NC_000925), brown algae *Odontella sinensis* (NC_001713), cryptonomad alga *Guillardia theta* (NC_000926), and from cyanobacterial genomes *Synechocystis* sp. PCC 6803 (NC_000911), *Synechococcus* sp. PCC 7002(AF052290), Anaebena (*Nostoc* ) sp. PCC 7120 (NC_0037272), *Nostoc punctiforme*, *Prochlorococcus marinus* MED4 (see draft genomes for the sequences of the later two at http://www.jgi.doe.gov/JGI_microbial/html/index.html) were aligned using CLUSTALW algorithm (Blosum62 scoring matrix) in Bioedit software (http://www.mbio.ncsu.edu/BioEdit/bioedit.html). The alignment was edited in the GeneDoc multiple alignment editor software (http://www.psc.edu/biomed/genedoc/). Amino-acids conserved in all sequences are shaded red and those conserved in the majority of the sequences are shaded blue. Location of transmembrane (TM) domains predicted by PHD algorithm (http://www.embl-heidelberg.de/predictprotein/predictprotein.html) are underlined (*). Sites of *phoA* and *LacZ* fusions constructs are marked with arrows above sequences. Functionally essential histidine (H274 in *C. reinhardtii*) is highlighted in green. Three blocks of conserved sequences in the predicted soluble in the predicted soluble lumenal domain are marked below the sequences as with 1, 2 and 3 respectively. Mature portion of *Oryza* Ccs1 protein was predicted based on BLAST result of translated genomic fragment OSM132311(courtesy of Monsanto rice-research.org queried against *Arabidopsis* Ccs1. Junction of splice site was predicted using NetPlantGene (http://www.cbs.dtu.dk/services/NetPGene/). N-terminal transit peptide region could not be predicted due to low homology and lack of predicted splice sites

**Supplemental Table I.**
**Primers used for amplification of *C. reinhardtii Ccs1***

| Primer | Position in genomic sequence[a] | Sequence (5' –3')[b] |
|---|---|---|
| 1 | –206 to –190 | CACATACGACCCCAAGC |
| 2 | +2169 to +2154 | GCAGGTACCGTCATGC |
| 3 | +2852 to +2868 | CACAGGGCGTCACCATG |
| 4 | +4357 to +4341 | CCTTCCCAAGTTCCACG |
| 5 | +1240 to +1255 | CAGCCGAAGTCGCTGC |
| 6 | +1892 to +1873 | GTGAACTTGTTGACGTGGAT |
| 7 | +3938 to +3953 | GGCGAAGCAGTAGGG |
| 8 | +1741 to +1724 | CATAGCAAGCACTCGGAG |
| 9 | +916 to +932 | TGACCCTACAGCTGGAC |
| 10 | +956 to +938 | GAAATAGTCAGCGGTGTAG |
| 11 | +3364 to +3381 | CAGTCGGTGGTGTTCTAC |
| 12 | +3443 to +3426 | TCCACCTCGATTGGCTTG |
| 13 | +728 to +747 | GTACCGCAACCAGGCACCTA |
| 14 | +1255 to +1240 | GCAGCGACTTCGGCTG |
| 15 | +323 to +343 | CAAGAAGAAGCTCAACGTGAC |
| 16 | +1406 to +1389 | TCAGCAGCGACGGACTGA |
| 17 | +1977 to +1995 | CATTCCTGCGATAGTGTTG |
| 18 | +3173 to +3157 | CCTGCAGCCAGCACTAC |
| 20 | +3237 to +3218 | AGCTCAAATTGTCAGTACAC |
| C199A-1 | +981 to +1013 | GCCTCCCTGGC**cg**C**ggc**CACCTACACCCGCCAG |
| C199A-2 | +1013 to +981 | CTGGCGGGTGTAGGTG**gcc**G**cg**GCCAGGGAGGC |
| H274A-1 | +1499 to +1530 | GGCCCATCGGCGTG**gc**CGCGGCGCTGCTGCTG |
| H274A-2 | +1530 to +1499 | CAGCAGCAGCGCCGCG**gc**CACGCCGATGGGCC |
| D348A-1 | +2042 to +2071 | CCGCAGTTCTAC**agc**G**ct**TTGTCGCTGCTT |
| D348A-2 | +2071 to +2042 | AAGCAGCGACAA**ag**C**gct**GTAGAACTGCGG |
| TRX5'[c] | +1801 to +1818 | TAGGTACCAGACTTCCAGGTGGTGGCTTC |
| TRX3'[c] | +3441 to +3426 | TAGGATCCCACCTCGATTGGCTTG |

[a] Numbering of the genomic DNA sequence defined as position +1 representing the start of translation.

[b] Lowercase, bold nucleotides indicate mutations

[c] Primers Trx5' and Trx3' designed with *Kpn*I and *Bam*HI restriction sites at the 5' ends of the primers, respectively, to facilitate cloning in-frame into the thioredoxin fusion expression vector pTrxFus.

**Supplemental Table II.**
**Primers used for amplification of *Synechocystis* sp. PCC6803 *Ccs1* for topology analysis**

| Primer | Sequence (5' –3') |
|---|---|
| R-ccsB23 | ACGCGTCGACAGGGTTTTGAGGCACTGC |
| R-ccsB67 | ACGCGTCGACCCAAATAGAGCTGGATCTTC |
| R-ccsB134 | ACGCGTCGAAAAACTTAAAGCTAG |
| R-ccsB225 | ACGCGTCGACTTGGGAATTTGACTGTCG |
| R-ccsB288 | ACGCGTCGACCCCGCAATGCCCCAGTTAG |
| R-ccsB349 | ACGCGTCGACAAATTGCCCTCTTGGTC |
| R-ccsB416 | ACGCGTCGACCCATCAACGCTCAATAAC |
| R-ccsB458 | ACGCGTCGACGCATTAACTTTAGCTTCTG |
| F-ccsBSac | TGTGAGCTCTTTCATGACCATTGC |
| F-ccsBNde | TTTGCCCAACATATGATTCCCAGTGGT |
| LacPstI | GTTGCTGCAGTTTGGAACAAG |